PHYSICAL REVIEW D **79,** 105012 (2009)

Inhomogeneous condensates in the thermodynamics of the chiral NJL_2 model

Gökçe Başar,[1] Gerald V. Dunne,[1] and Michael Thies[2]

[1]*Physics Department, University of Connecticut, Storrs, Connecticut 06269, USA*

[2]*Institut für Theoretische Physik, Universität Erlangen-Nürnberg, D-91058, Erlangen, Germany*

(Received 10 March 2009; published 14 May 2009)

We analyze the thermodynamical properties, at finite density and nonzero temperature, of the $(1 + 1)$ dimensional chiral Gross-Neveu model (the NJL_2 model), using the exact inhomogeneous (crystalline) condensate solutions to the gap equation. The continuous chiral symmetry of the model plays a crucial role, and the thermodynamics leads to a broken phase with a periodic spiral condensate, the ''chiral spiral,'' as a thermodynamically preferred limit of the more general ''twisted kink crystal'' solution of the gap equation. This situation should be contrasted with the Gross-Neveu model, which has a discrete chiral symmetry, and for which the phase diagram has a crystalline phase with a periodic kink crystal. We use a combination of analytic, numerical, and Ginzburg-Landau techniques to study various parts of the phase diagram.

DOI: 10.1103/PhysRevD.79.105012 PACS numbers: 11.10.Kk, 11.10.Wx, 11.30.Rd, 71.10.Pm

I. INTRODUCTION

The phase diagram of interacting fermion systems at finite density and temperature is a general problem with applications in a wide range of physical contexts. Well-studied examples include the Peierls-Frohlich model of conduction [1], the Gorkov-Bogoliubov-de Gennes approach to superconductivity [2], and the Nambu-Jona-Lasinio (NJL) model of symmetry breaking in particle physics [3]. Strongly interacting theories such as quantum chromodynamics (QCD) exhibit a rich phase diagram structure [4–6]. It is known that chiral symmetry plays a key role, and computationally the large N_f and large N_c limits must be addressed carefully [7,8]. A $(1 + 1)$-dimensional version of the NJL model, the NJL_2 model [also known as the *chiral* Gross-Neveu model, $\chi\mathrm{GN}_2$] is of interest because it captures some important features of QCD, such as asymptotic freedom, dynamical mass generation, a large N_f limit, and the breaking of a continuous chiral symmetry [9–12]. In this paper, we use the exact crystalline solutions to the associated gap equation, found recently in [13,14], to study the temperature-density phase diagram of this NJL_2 system. The result of our thermodynamical analysis confirms the physical picture proposed in [15] that there is a phase transition at a critical temperature T_c from a massless phase to a broken phase with a helical condensate (the ''chiral spiral''), of the complex Larkin-Ovchinikov-Fulde-Ferrell (LOFF) form. The resulting phase diagram (see below, Fig. 5), is very different from that of the nonchiral Gross-Neveu (GN_2) model, which has just a discrete, rather than continuous, chiral symmetry. In the GN_2 model there is also a region of the phase diagram with a crystalline order parameter [16], but the structure of the phase diagram is very different (see below, Fig. 7). This crystalline phase of GN_2 has been clearly seen in a recent lattice analysis [17], extending an important earlier lattice analysis [18]. In this paper, we explain in detail the role of the chiral symmetry (continuous versus discrete) in determining the form of the phase diagram. The chiral spiral phase of the NJL_2 model has also been studied in the anti-de Sitter/QCD framework [19]. These one dimensional models are of course simplified models of more realistic $(3 + 1)$-dimensional systems, but important lessons can still be learned concerning the appearance of crystalline structures in the phase diagram [20,21]. Furthermore, their solubility permits a detailed study of the relation between real and imaginary chemical potential [22].

Our analysis is ultimately based on solving the gap equation for inhomogeneous condensates. Initially, the phase diagram of the NJL_2 and GN_2 models was studied assuming homogeneous condensates [23,24], but this assumption does not capture certain aspects of the true physical phase diagram [16–18]. Of course, finding inhomogeneous solutions to the gap equation is a much more difficult technical problem, but the massless NJL_2 and GN_2 models have remarkable symmetry properties that enable one to find the general periodic condensate solutions [13,14]. This fact is due to a deep connection between the Bogoliubov-de Gennes effective Hamiltonian of the NJL_2 system, and certain one dimensional integrable hierarchies [25–27]. These exact solutions are characterized by a finite number of parameters, and to describe the phase diagram one must minimize the thermodynamical grand potential with respect to these parameters in order to determine the form of the condensate in a given region of the (T, μ) plane. This thermodynamical analysis is performed in this paper.

In Sec. II, we briefly review the analytical solution of the inhomogeneous gap equation. In Sec. III, we identify the special role played by rescaling and phase rotation symmetries in the NJL_2 model. The thermodynamics of the NJL_2 model is discussed in terms of a spiral condensate in Sec. IV and in terms of the general twisted kink crystal in Sec. V. In Sec. VI, we contrast this analysis with the case of

the GN_2 model, which has just a discrete chiral symmetry. In Sec. VII, we apply a Ginzburg-Landau analysis to study the region of the phase diagrams of both the GN_2 and NJL_2 models, in the vicinity of the relevant "tricritical point." We conclude with a summary of our results and a discussion of the implications for more complicated models.

II. SOLVING THE INHOMOGENEOUS GAP EQUATION

The NJL_2 model is described by the following $(1+1)$-dimensional Lagrangian with both scalar and pseudoscalar four-fermion interaction terms:

$$\mathcal{L}_{\mathrm{NJL}} = \bar{\psi} i\partial\!\!\!/ \psi + \frac{g^2}{2}[(\bar{\psi}\psi)^2 + (\bar{\psi} i\gamma^5 \psi)^2]. \tag{2.1}$$

This model has a continuous chiral symmetry: $\psi \to e^{i\gamma^5\alpha}\psi$. The GN_2 model has just the scalar four-fermion interaction term:

$$\mathcal{L}_{\mathrm{GN}} = \bar{\psi} i\partial\!\!\!/ \psi + \frac{g^2}{2}[(\bar{\psi}\psi)^2], \tag{2.2}$$

and has a discrete chiral symmetry: $\psi \to \gamma^5\psi$. We study these models in the large N_f limit where the semiclassical approximation applies and chiral symmetry breaking can be studied [28,29].

By a Hubbard-Stratonovich transformation, the four-fermion interaction terms can be expressed in terms of scalar and pseudoscalar bosonic condensate fields, Σ and Π (respectively), which are conveniently expressed in terms of a complex condensate field: $\Delta = \Sigma - i\Pi$. For GN_2 we only have Σ, and so the condensate field Δ is real. The general NJL_2 system can be described equivalently by the effective Lagrangian:

$$\mathcal{L} = \bar{\psi}\left[i\partial\!\!\!/ - \frac{1}{2}(1-\gamma^5)\Delta - \frac{1}{2}(1+\gamma^5)\Delta^*\right]\psi - \frac{1}{2g^2}|\Delta|^2, \tag{2.3}$$

which is now quadratic in the fermion fields. The corresponding single-particle fermionic Hamiltonian is

$$H = -i\gamma^5\frac{d}{dx} + \gamma^0\left(\frac{1}{2}(1-\gamma^5)\Delta + \frac{1}{2}(1+\gamma^5)\Delta^*\right). \tag{2.4}$$

With the choice of the Dirac matrices as $\gamma_0 = \sigma_1$, $\gamma_1 = -i\sigma_2$, and $\gamma^5 = \sigma_3$, the Hamiltonian (2.4) takes the form:

$$H = \begin{pmatrix} -i\frac{d}{dx} & \Delta(x) \\ \Delta^*(x) & i\frac{d}{dx} \end{pmatrix}. \tag{2.5}$$

This Hamiltonian is also known as the Bogoliubov-de Gennes (BdG) (or Andreev) Hamiltonian in the superconductivity literature [2,30].

There are two equivalent perspectives on studying the semiclassical gap equation for static condensates. The first, a Hartree-Fock approach, is to solve the single-particle equation (the Bogoliubov-de Gennes equation)

$$H\psi = E\psi \tag{2.6}$$

subject to the consistency condition relating the condensate field to the expectation values of the scalar and pseudoscalar fermionic bilinears:

$$\langle\bar{\psi}\psi\rangle - i\langle\bar{\psi} i\gamma^5\psi\rangle = -\Delta/g^2. \tag{2.7}$$

This gap equation is obtained by varying the effective action (per fermion flavor) and is exact at large N_f. In this second, functional, approach one integrates out the fermionic field in (2.3) and obtains an effective action (per fermion flavor) for the condensate field:

$$S_{\mathrm{eff}}[\Delta] = -\frac{1}{2g^2N_f}\int d^2x|\Delta|^2 - i\ln\det\left[i\partial\!\!\!/ - \frac{1}{2}(1-\gamma^5)\Delta - \frac{1}{2}(1+\gamma^5)\Delta^*\right]. \tag{2.8}$$

The gap equation for the condensate field is obtained by varying with respect to $\Delta^*(x)$ to find the stationary points of $S_{\mathrm{eff}}[\Delta]$:

$$0 = \frac{\delta S_{\mathrm{eff}}}{\delta\Delta^*} = -\frac{1}{2g^2N_f}\Delta(x) - i\frac{\delta}{\delta\Delta(x)^*}\ln\det\left[i\partial\!\!\!/ - \frac{1}{2}(1-\gamma^5)\Delta(x) - \frac{1}{2}(1+\gamma^5)\Delta(x)^*\right]. \tag{2.9}$$

It is straightforward to solve this gap equation when the condensate field Δ is uniform, but it is more technically challenging to solve it for an inhomogeneous condensate field $\Delta(x)$. Nevertheless, in one spatial dimension it is possible to find the most general bounded quasiperiodic solution to this gap equation [13,14]. The general solution has the form of a "twisted kink crystal," described below.

A useful quantity for solving the inhomogeneous gap equation (2.9) is the resolvent $R(x;E)$, the coincident-point limit of the Gor'kov Green's function $G(x,y;E)$ corresponding to the Hamiltonian (2.5)

$$R(x;E) \equiv \left\langle x\left|\frac{1}{H-E}\right|x\right\rangle. \tag{2.10}$$

For a *static* condensate the gap eq. (2.9) can be written as

$$\Delta(x) = -iN_f g^2 \mathrm{tr}_{D,E}[\gamma^0(\mathbf{1}+\gamma^5)R(x;E)] \tag{2.11}$$

The solution of the gap equation relies on the remarkable fact that in one spatial dimension the resolvent (itself a 2×2 matrix) must satisfy a simple first order matrix differential equation

$$\frac{\partial}{\partial x}R(x;E)\sigma_3 = i\left[\begin{pmatrix} E & -\Delta(x) \\ \Delta^*(x) & -E \end{pmatrix}, R\sigma_3\right] \tag{2.12}$$

This equation is known as the Eilenberger equation in the superconductivity literature [30,31], and as the Dickey equation in mathematical physics [26,32]. The Dickey-Eilenberger equation follows immediately from the fact that the resolvent can be written as a product of two linearly independent solutions:

$$R(x;E) = \frac{1}{2iW}(\psi_1\psi_2^T + \psi_2\psi_1^T)\sigma_1 \tag{2.13}$$

where $W = i(\psi_1^T\sigma_2\psi_2)$ is the Wronskian of two independent solutions $\psi_{1,2}$ of $H\psi = E\psi$.

The inhomogeneous gap Equation (2.9) can be solved by the following simple ansatz [13,14] for the resolvent

$$R(x;E) = \mathcal{N}(E)\begin{pmatrix} a(E) + |\Delta|^2 & b(E)\Delta - i\Delta' \\ b(E)\Delta^* + i\Delta^{*\prime} & a(E) + |\Delta|^2 \end{pmatrix} \tag{2.14}$$

where $\mathcal{N}(E)$, $a(E)$, and $b(E)$ are functions of the energy E, and are to be determined. This particular ansatz is motivated by the gap equation (2.11) that relates the off diagonal component of the resolvent with Δ. The ansatz (2.14) automatically solves the diagonal part of the Eilenberger equation (2.12), while the off diagonal part requires that the condensate field Δ satisfy the complex nonlinear Scrödinger equation (NLSE):

$$\Delta'' - 2|\Delta|^2\Delta + i(b(E) - 2E)\Delta' - 2(a(E) - Eb(E))\Delta = 0. \tag{2.15}$$

The advantage of this ansatz approach is that the NLSE (2.15) can be solved in closed form, and its general solution has the form of a twisted kink crystal, described in detail in [14] and summarized below in the next section. The associated energy functions $\mathcal{N}(E)$, $a(E)$, and $b(E)$ are simple functions of E. For the NJL$_2$ model, there is a further consistency condition required to satisfy the gap equation (2.11): for an inhomogeneous condensate, the part of the off diagonal resolvent proportional to $\Delta'(x)$ must vanish. This is explained in detail in Sec. VI.A of [14], in particular, Eq. (6.2). Here we work at finite temperature and nonzero density, which simply changes the meaning of the energy trace, to include a Fermi-Dirac factor, when computing the effective action. Thus, we obtain a condition on the energy function $\mathcal{N}(E)$:

$$0 = \mathrm{tr}_E(\mathcal{N}(E)) \equiv \int \frac{dE}{2\pi}\frac{\mathcal{N}(E)}{1 + e^{\beta(E-\mu)}}. \tag{2.16}$$

Here $\beta = 1/T$ is the inverse temperature and μ is the chemical potential. This consistency condition imposes one relation on the parameters describing the twisted kink solution. With this consistency condition imposed, the general inhomogeneous condensate $\Delta(x)$ satisfying the NLSE (2.15) solves the gap equation (2.9).

Given this exact solution $\Delta(x)$ to the gap equation (2.9), it is also possible to find the exact single-particle solutions to the BdG equation (2.6). Furthermore, the diagonal resolvent $R(x;E)$ in (2.14) encodes all the relevant spectral information. For example, the local density of states for fermions in the presence of the condensate is given by

$$\rho(x;E) = \frac{1}{\pi}\,\mathrm{Im}\,\mathrm{tr}_D(R(x;E + i\epsilon)) \tag{2.17}$$

where the matrix trace of the resolvent follows trivially from the ansatz (2.14):

$$\mathrm{tr}_D(R(x;E)) = 2\mathcal{N}(E)(a(E) + |\Delta(x)|^2). \tag{2.18}$$

Given the density of states $\rho(E) = \int dx\rho(x;E)$, all relevant thermodynamic quantities, at finite temperature and chemical potential, can be derived from the grand canonical potential

$$\Psi[\Delta(x);T,\mu] = -\frac{1}{\beta}\int_{-\infty}^{\infty} dE\rho(E)\ln(1 + e^{-\beta(E-\mu)}) + \frac{1}{2N_f g^2}\frac{1}{L}\int_0^L dx|\Delta(x)|^2. \tag{2.19}$$

Since we know $\rho(E)$ exactly, we can analyze the thermodynamical properties of this model precisely.

A. Twisted kink crystal condensate

The general solution to the NLSE (2.15) describes a crystalline condensate [13,14]. It is a periodic array of kinks that also rotate in the chiral plane, as illustrated in Fig. 1. The *single* chirally-twisted kink was originally found by Shei [11] using inverse scattering techniques, and subsequently studied in a resolvent approach by Feinberg and Zee [12]. The periodic array of such twisted kinks can be expressed in terms of the elliptic functions:

$$\Delta(x) = -\lambda e^{2iqx}A\frac{\sigma(\lambda Ax + i\mathbf{K}' - i\theta/2)}{\sigma(\lambda Ax + i\mathbf{K}')\sigma(i\theta/2)} \times \exp[i\lambda Ax(-i\zeta(i\theta/2) + i\,\mathrm{ns}(i\theta/2)) + i\theta\eta_3/2] \tag{2.20}$$

where $\mathrm{sc} = \mathrm{sn}/\mathrm{cn}$, $\mathrm{nd} = 1/\mathrm{dn}$ are Jacobi elliptic functions, and the functions σ and ζ are the Weierstrass sigma and zeta functions [33], chosen to have real and imaginary half periods: $\omega_1 = \mathbf{K}(\nu)$, and $\omega_3 = i\mathbf{K}' \equiv i\mathbf{K}(1-\nu)$. Here $\mathbf{K}(\nu) = \int_0^{\pi/2} dt/\sqrt{1 - \nu\sin^2 t}$ is the complete elliptic integral, and we use the standard notation that $\mathbf{K}'(\nu) \equiv \mathbf{K}(1-$

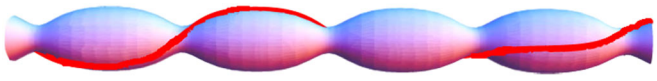

FIG. 1 (color online). The twisted kink crystal condensate of (2.20), shown as the solid (red) curve. The (blue) skeleton surface is shown just to illustrate the periodic amplitude modulation and phase winding.

ν). Both periods are therefore controlled by a single (real) elliptic parameter $0 \le \nu \le 1$. Note that $\eta_3 = \zeta(i\mathbf{K}')$ is purely imaginary. The parameter λ sets the overall scale of the condensate, and $1/\lambda$ sets the length scale of the crystal. Later, we will use units in which the vacuum mass of the fermion is 1, so that λ sets the scale relative to the vacuum fermion mass. The angular parameter θ takes values in the range $\theta \in [0, 4\mathbf{K}'(\nu)]$. The (real) constant A is a function of θ and the elliptic parameter ν:

$$A = A(\theta, \nu) = -2i\,\mathrm{sc}(i\theta/4; \nu)\,\mathrm{nd}(i\theta/4; \nu). \tag{2.21}$$

For brevity we will usually suppress the explicit dependence of the elliptic functions on the elliptic parameter ν. The final parameter q is a phase parameter that affects the chiral angle through which the condensate rotates over one period $L = \frac{2\mathbf{K}}{\lambda A}$:

$$\Delta(x + L) = e^{2i\varphi}\Delta(x);$$
$$\varphi = \mathbf{K}\left(-i\zeta(i\theta/2) + i\,\mathrm{ns}(\theta/2) - \frac{\eta\theta}{2\mathbf{K}} + \frac{2q}{\lambda A}\right) \tag{2.22}$$

where $\eta \equiv \zeta(\mathbf{K})$ is real. Thus the general solution is specified by four real parameters: a scale parameter λ, a phase parameter q, an angular parameter θ, and the elliptic parameter ν. These parameters also parametrize the energy spectrum of fermions in such a condensate background, which has two gaps, with band edges $E_1 \le E_2 \le E_3 \le E_4$ as shown in the first plot of Fig. 2:

$$\begin{aligned} E_1 &= q - \lambda \qquad E_2 = q + \lambda(-1 + 2\,\mathrm{nc}^2(i\theta/4)) \\ E_3 &= q + \lambda(-1 + 2\,\mathrm{nd}^2(i\theta/4)) \qquad E_4 = q + \lambda. \end{aligned} \tag{2.23}$$

Thus, in terms of the single-particle fermion spectrum, the role of the four parameters is as follows: λ determines the overall energy scale; q determines the overall offset; while θ and ν determine the location and width of the band that lies in the gap between the "outer" edges E_1 and E_4. The simple linear dependence of the energy spectrum on the parameters λ and q is a direct consequence of the form of the Hamiltonian (2.5), and reflects the important scale and shift symmetry described in detail in Sec. III.

For the twisted kink crystal solution (2.20), the coefficients $a(E)$ and $b(E)$ in the NLSE (2.15) are simple polynomials of E, with coefficients determined by the band edges:

$$a(E) = 2E^2 - \left(\sum_{j=1}^{4} E_j\right)E + \frac{1}{8}\left\{\left(\sum_{j=1}^{4} E_j\right)^2 - \sum_{i<j}^{4}(E_i - E_j)^2\right\} \tag{2.24}$$

$$b(E) = 2E - \left(\sum_{j=1}^{4} E_j\right). \tag{2.25}$$

Furthermore, the energy function $\mathcal{N}(E)$ appearing in the resolvent ansatz (2.14) also has a very simple form in terms of the band edges:

$$\mathcal{N}(E) = \frac{i}{4\sqrt{\prod_{j=1}^{4}(E - E_j)}}. \tag{2.26}$$

Thus, we have an explicit exact expression for the density of states of fermions in the presence of such a twisted kink condensate field, following from the trace of the resolvent. Within the bands:

$$\rho(E) = \frac{1}{2\pi}\frac{a(E) + \lambda^2 Z}{\sqrt{\prod_{j=1}^{4}(E - E_j)}}. \tag{2.27}$$

Here we have defined the function $Z(\theta, \nu)$ in terms of the normalized average of $|\Delta(x)|^2$ over one period:

$$Z(\theta, \nu) \equiv \frac{1}{\lambda^2}\langle|\Delta(x)|^2\rangle = -A(\theta, \nu)^2\left(\mathcal{P}(i\theta/2) + \frac{\eta}{\mathbf{K}}\right) \tag{2.28}$$

with $\mathcal{P}$ being the Weierstrass $\mathcal{P}$ function. Thus, the density of states $\rho(E)$ is an explicitly known function of the energy E, depending parametrically on the four parameters λ, q, θ, and ν that characterize the solution (2.20) to the gap

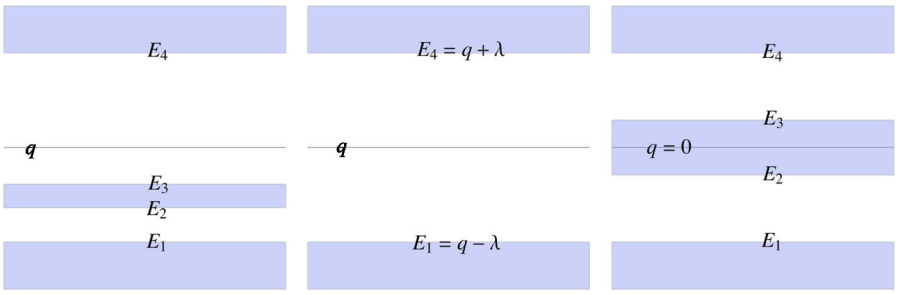

FIG. 2 (color online). The form of the single-particle fermion spectra for the general twisted kink crystal (first figure), showing the central value $E = q$, and the band edges E_j, for $j = 1 \ldots 4$. The second figure shows the special case of the spiral condensate, for which the bound band merges with one of the continua. The third figure shows the spectrum for another special case, the real kink crystal, which has a charge-conjugation symmetry, implying that the offset is $q = 0$, and the spectrum is symmetric about 0. The position of the bands within the gap, and their width, are controlled by the parameters θ and ν.

equation. This parametric dependence enters through the band edge energies E_j in (2.23), and through the function Z defined in (2.28).

B. Spiral condensate

An important special case of the general solution (2.20) is the degenerate case when the bound band of the fermion spectrum shrinks and merges with the upper or lower continuum, so that the spectrum has just a single gap, as shown in the second plot in Fig. 2. This occurs when the angular parameter takes values at its extreme limits: $\theta = 0$ (which implies that $E_2 = E_3 = E_4$, so that the bound band merges with the upper continuum), or $\theta = 4\mathbf{K}'$ (which implies that $E_1 = E_2 = E_3$, so that the bound band merges with the lower continuum). The general twisted kink crystal condensate (2.20) reduces to a single plane wave

$$\Delta = \lambda e^{2iqx} \tag{2.29}$$

which is clearly a solution to the NLSE (2.15). For this condensate the amplitude is constant, while the phase rotates at a constant rate, set by q, as shown in Fig. 3. The fermion energy spectrum has just one gap, of width 2λ, centered at q; that is, the band edges lie at $E_1 = q - \lambda$, and $E_4 = q + \lambda$. Correspondingly, the resolvent trace has a simplified form, and the spectral function within the continuum bands is simply:

$$\rho(E) = \frac{1}{\pi}\frac{|E-q|}{\sqrt{\lambda^2 - (E-q)^2}} \tag{2.30}$$

which we recognize as the spectral function of a constant condensate $\Delta = \lambda$, shifted in energy by q.

C. Real kink crystal

Another important special case of the general solution (2.20) is the case where the condensate is real (relevant for the GN_2 model), which implies that the BdG Hamiltonian H in (2.5) has a charge-conjugation symmetry, $\{H, \sigma_2\} = 0$, which in turn implies that the fermionic spectrum is symmetric, as shown in the third plot of Fig. 2. The band edges reduce to

$$E_1 = -\lambda = -E_4 \qquad E_2 = -\lambda\left(\frac{1-\sqrt{\nu}}{1+\sqrt{\nu}}\right) = -E_3. \tag{2.31}$$

The phase parameter $q = 0$, and further the angular parameter θ takes its midpoint value $\theta = 2\mathbf{K}'(\nu)$. Thus the real kink crystal is described by just two parameters, the scale λ and the elliptic parameter ν:

$$\begin{aligned}\Delta(x) &= \lambda\left(\frac{2\sqrt{\nu}}{1+\sqrt{\nu}}\right)\mathrm{sn}\left(\frac{2\lambda x}{1+\sqrt{\nu}};\nu\right)\\ &= \lambda\tilde{\nu}\frac{\mathrm{sn}(\lambda x;\tilde{\nu})\,\mathrm{cn}(\lambda x;\tilde{\nu})}{\mathrm{dn}(\lambda x;\tilde{\nu})};\\ \tilde{\nu} &\equiv \frac{4\sqrt{\nu}}{(1+\sqrt{\nu})^2}.\end{aligned} \tag{2.32}$$

The second form of $\Delta(x)$ in (2.32) is obtained from the first form by a Landen transformation [33]. Over one period, $L = \frac{2\mathbf{K}(\tilde{\nu})}{\lambda}$, the condensate changes sign (that is, it rotates through an angle $2\varphi = -\pi$), as shown in Fig. 4. This change of sign corresponds to the *discrete* chiral symmetry of the GN_2 model, while the phase rotation (2.22) of the general kink crystal condensate (2.20) is associated with the *continuous* chiral symmetry of the NJL_2 model. The real kink crystal describes the inhomogeneous condensate of the crystalline phase of the GN_2 model [16], and its thermodynamics will be discussed below in Sec. VI.

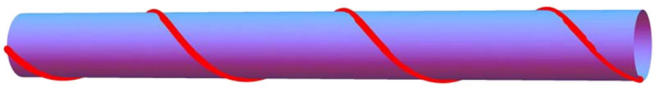

FIG. 3 (color online). The spiral condensate of (2.29), shown as the solid (red) curve. The (blue) skeleton surface is shown just to illustrate the periodic phase winding. In contrast to the twisted kink crystal in Fig. 1, for the spiral, the amplitude is constant.

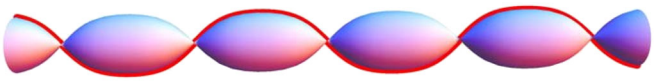

FIG. 4 (color online). The real kink crystal condensate of (2.32), shown as the solid (red) curve. The (blue) skeleton surface is shown just to illustrate the periodic amplitude modulation and phase winding. For this real kink crystal, the amplitude vanishes each period, and the kink rotates through π (i.e., changes sign) each period.

III. THE SCALE AND PHASE SYMMETRY IN NJL_2

In this section, we describe a simple but important symmetry property of the Bogoliubov-de Gennes equation (2.6), that has important consequences for the thermodynamical analysis. The Bogoliubov-de Gennes equation (2.6) admits a family of solutions obtained by rescaling and phase shifting (i.e., making a *linear* local chiral rotation) a given solution:

$$\Delta(x) \to \lambda\Delta(\lambda x)e^{2iqx} \qquad \psi(x) \to e^{iqx\gamma_5}\lambda^{1/2}\psi(\lambda x) \tag{3.1}$$

which generates all the linear transformations acting on the energy spectrum:

$$E \to \lambda E + q. \tag{3.2}$$

In terms of the density of states, the effect of the transformation is

$$\rho(E) \to \rho\left(\frac{E-q}{\lambda}\right). \tag{3.3}$$

The important physical implication of this symmetry is that when minimizing the grand potential (2.19) with respect to

the four parameters λ, q, θ, and ν, the minimization with respect to λ and q can be done first. If the grand potential did not require renormalization, then the minimization with respect to λ and q would be trivial. In fact, we will show in the next section that even taking into account the renormalization, these symmetries greatly simplify the minimization with respect to λ and q.

It is useful to define the "unscaled" and "unshifted" spectrum to be the one with $\lambda = 1$ and $q = 0$, so that $E_1 = -1$, and $E_4 = 1$ (in units where the vacuum fermion mass is 1). All other spectral functions can be generated from this basic solution using the simple transformation (3.3). The corresponding density of states will be written as

$$\hat{\rho}(E) = \frac{1}{2\pi} \times \frac{(2E^2 - (\hat{E}_2 + \hat{E}_3)E - (\hat{E}_3 - \hat{E}_2)^2/4 - 1 + Z)}{\sqrt{(E^2 - 1)(E - \hat{E}_2)(E - \hat{E}_3)}} \tag{3.4}$$

where $Z = Z(\theta, \nu)$ is defined in (2.28), and

$$\begin{aligned} \hat{E}_2 &= -1 + 2\,\mathrm{nc}^2(i\theta/4; \nu) \\ \hat{E}_3 &= -1 + 2\,\mathrm{nd}^2(i\theta/4; \nu). \end{aligned} \tag{3.5}$$

Importantly, $\hat{\rho}(E)$ depends parametrically only on the two remaining parameters, θ and ν. This separation of parametric dependences has important consequences for the minimization of the thermodynamic grand potential (2.19) with respect to the parameters.

A. Transformation properties of thermodynamic quantities

1. The grand potential Ψ

We begin our discussion with the grand canonical potential $\Psi[\hat{\Delta}(x); T, \mu]$ for the unscaled/unshifted condensate $\hat{\Delta}(x)$, obtained from (2.20) by setting the scale parameter $\lambda = 1$, and the phase parameter $q = 0$. The grand potential is formally divergent in the UV region and has to be renormalized, as is well known [9,10,16]. At finite density and nonzero temperature, it is convenient to separate the single-particle contribution as

$$\begin{aligned} -\frac{1}{\beta}\int_{-\infty}^{\infty} dE\hat{\rho}(E)\ln(1 + e^{-\beta(E-\mu)}) &= \int_{E_{\min}}^{\mu} dE\hat{\rho}(E)(E - \mu) \\ &\quad - \frac{1}{\beta}\int_{-\infty}^{\infty} dE\hat{\rho}(E)\ln(1 + e^{-\beta|E-\mu|}) \end{aligned} \tag{3.6}$$

where $E_{\min} = -\Lambda/2 - Z/\Lambda + \ldots$, in terms of the momentum cutoff $\Lambda/2$. Only the first term, the zero temperature expression, in (3.6) is divergent. We isolate the divergent terms using the large E behavior of the density of states (3.4):

$$\hat{\rho}(E) \approx 1 + \frac{Z}{2E^2} + \ldots \tag{3.7}$$

The divergent part is

$$\Psi_{\mathrm{div}} = -\frac{\Lambda^2}{8\pi} - \frac{\Lambda\mu}{2\pi} - \frac{Z}{2\pi}\ln\Lambda. \tag{3.8}$$

The quadratically and linearly divergent terms are absorbed by definition of the renormalized energy and baryon number densities, and the logarithmically divergent term is canceled by the double counting correction [16]

$$\frac{1}{2N_f g^2}\frac{1}{L}\int_0^L |\hat{\Delta}(x)|^2 dx = \frac{Z}{2\pi}\ln\Lambda \tag{3.9}$$

where we have used the vacuum gap equation $\frac{\pi}{N_f g^2} = \ln\Lambda$. Hence the finite renormalized grand canonical potential is

$$\begin{aligned} \Psi_{\mathrm{ren}}[\hat{\Delta}(x); T, \mu] &= \int_{E_{\min}}^{\mu} dE\hat{\rho}(E)(E - \mu) \\ &\quad - \frac{1}{\beta}\int_{-\infty}^{\infty} dE\hat{\rho}(E)\ln(1 + e^{-\beta|E-\mu|}) \\ &\quad + \frac{\Lambda^2}{8\pi} + \frac{\Lambda\mu}{2\pi} + \frac{Z}{2\pi}\ln\Lambda. \end{aligned} \tag{3.10}$$

Now we can analyze the effect of the transformation (3.3) on the *renormalized* grand canonical potential for the general condensate

$$\Delta(x) = \lambda\hat{\Delta}(\lambda x)e^{2iqx}. \tag{3.11}$$

The finite temperature (FT) contribution [the 2nd term on the right-hand side of Eq. (3.10)] has the following simple scaling behavior,

$$\begin{aligned} \Psi_{\mathrm{ren}}[\lambda\hat{\Delta}(\lambda x)e^{2iqx}; T, \mu]|_{\mathrm{FT}} &= -\frac{1}{\beta}\int_{-\infty}^{\infty} dE\hat{\rho}\left(\frac{E - q}{\lambda}\right) \\ &\quad \times \ln(1 + e^{-\beta|E-\mu|}) \\ &= -\frac{\lambda^2}{\hat{\beta}}\int_{-\infty}^{\infty} dE\hat{\rho}(E) \\ &\quad \times \ln(1 + e^{-\hat{\beta}|E-\hat{\mu}|}) \\ &= \lambda^2\Psi_{\mathrm{ren}}[\hat{\Delta}(x); \hat{T}, \hat{\mu}]|_{\mathrm{FT}} \end{aligned} \tag{3.12}$$

with the rescaled variables

$$\hat{\mu} = \frac{\mu - q}{\lambda} \qquad \hat{\beta} = \frac{1}{\hat{T}} = \lambda\beta. \tag{3.13}$$

For the zero temperature contribution (ZT.) in (3.10), we start from the expression,

$$\Psi_{\rm ren}[\lambda\hat{\Delta}(\lambda x)e^{2iqx};T,\mu]|_{\rm ZT} = \int_{E^{\lambda}_{\rm min}}^{\mu} dE\hat{\rho}\left(\frac{E-q}{\lambda}\right)(E-\mu) + \frac{\Lambda^2}{8\pi} + \frac{\Lambda\mu}{2\pi} + \frac{\lambda^2 Z}{2\pi}\ln\Lambda \tag{3.14}$$

where $E^{\lambda}_{\rm min} = -\Lambda/2 - \lambda^2 Z/\Lambda$. Here, due to the regularization, the scaling relation analogous to Eq. (3.12) develops anomalous terms akin to the chiral U(1) and scale anomalies,

$$\Psi_{\rm ren}[\lambda\hat{\Delta}(\lambda x)e^{2iqx};T,\mu]|_{\rm ZT} = \lambda^2\Psi_{\rm ren}[\hat{\Delta}(x);\hat{T},\hat{\mu}]|_{\rm ZT} + \frac{Z}{2\pi}\lambda^2\ln\lambda + \lambda^2\frac{\hat{\mu}^2}{2\pi} - \frac{\mu^2}{2\pi}. \tag{3.15}$$

Being an UV effect, the extra terms are independent of temperature. Combining Eqs. (3.12) and (3.15), we see that the renormalized grand potential for the general condensate in (3.11) is

$$\Psi_{\rm ren}[\lambda\hat{\Delta}(\lambda x)e^{2iqx};T,\mu] = \lambda^2\left(\hat{\Psi}_{\rm ren} + \frac{Z}{2\pi}\ln\lambda + \frac{\hat{\mu}^2}{2\pi}\right) - \frac{\mu^2}{2\pi} \tag{3.16}$$

with the shorthand notation

$$\hat{\Psi}_{\rm ren} \equiv \Psi_{\rm ren}[\hat{\Delta}(x);\hat{T},\hat{\mu}]. \tag{3.17}$$

For the sake of compactness in the notation, we will drop the subscript "ren" from now on, and work exclusively with the physical renormalized thermodynamic quantities.

The grand canonical potential is related to the density ρ, [not to be confused with the density of states $\rho(E)$], the entropy s, and the free energy u:

$$\Psi = u - \mu\rho - Ts. \tag{3.18}$$

Thus we can obtain expressions for the effect of the scaling and phase shifting transformation on the renormalized ρ, s, and u as follows.

2. Number density

From the basic relation $\rho = -\frac{\partial\Psi}{\partial\mu}$, we write $\frac{\partial}{\partial\mu} = \frac{1}{\lambda}\frac{\partial}{\partial\hat{\mu}}$, and act on (3.16) to obtain

$$\rho = \lambda^2\left(-\frac{1}{\lambda}\frac{\partial\hat{\Psi}}{\partial\hat{\mu}} - \frac{1}{\lambda}\frac{\hat{\mu}}{\pi}\right) + \frac{\mu}{\pi} = \lambda\hat{\rho} + \frac{q}{\pi}. \tag{3.19}$$

3. Entropy

From the basic relation $s = -\frac{\partial\Psi}{\partial T}$, we write $\frac{\partial}{\partial T} = \frac{1}{\lambda}\frac{\partial}{\partial\hat{T}}$, and act on (3.16) to obtain

$$s = \lambda^2\left(-\frac{1}{\lambda}\frac{\partial\hat{\Psi}}{\partial\hat{T}}\right) = \lambda\hat{s}. \tag{3.20}$$

4. Free energy

The transformation property of the free energy now follows directly from the relation (3.18)

$$u = \Psi + \mu\rho + Ts = \lambda^2\left(\hat{u} + \frac{Z}{2\pi}\ln\lambda\right) + \lambda q\hat{\rho} + \frac{q^2}{2\pi}. \tag{3.21}$$

B. Implications for minimization of the grand potential Ψ with respect to the phase parameter q

The minimization of Ψ with respect to q can be transformed into minimization with respect to the chemical potential, due to the symmetry (3.3). We write $\frac{\partial}{\partial q} = -\frac{1}{\lambda}\times\frac{\partial}{\partial\hat{\mu}}$, and differentiate Ψ in (3.16) with respect to $\hat{\mu}$:

$$0 = -\frac{\partial\Psi}{\partial\hat{\mu}} = \lambda^2\left(-\frac{\partial\hat{\Psi}}{\partial\hat{\mu}} - \frac{\hat{\mu}}{\pi}\right) = \lambda^2\left(\hat{\rho} - \frac{\hat{\mu}}{\pi}\right), \tag{3.22}$$

so the q minimization implies

$$\pi\hat{\rho} = \hat{\mu}. \tag{3.23}$$

Recalling (3.19) and (3.13), this means that after minimizing with respect to the phase parameter q, the (period averaged) number density is simply proportional to the chemical potential:

$$\rho = \frac{\mu}{\pi}. \tag{3.24}$$

This remarkable fact is independent of the form of the (complex) condensate, and simply follows from the transformation property (3.1) of the BdG Hamiltonian and its effect on the renormalized grand potential, as reflected in (3.16). Note, of course, that such a relation between ρ and μ *does not arise* in the GN_2 model, where the condensate is real and there is no phase invariance parameter q.

C. Implications for minimization of the grand potential Ψ with respect to the scale parameter λ

From (3.16), it follows that Ψ depends on the scale λ explicitly, and also implicitly though the dependence of $\hat{\Psi} \equiv \Psi[\hat{\Delta};\hat{T},\hat{\mu}]$ on $\hat{T} = T/\lambda$, and on $\hat{\mu} = (\mu - q)/\lambda$. Thus we can write

$$\begin{aligned}\frac{\partial\Psi}{\partial\lambda} &= 2\lambda\left(\hat{\Psi} + \frac{Z}{2\pi}\ln\lambda\right) + \frac{Z\lambda}{2\pi} + \lambda^2\left(-\frac{\hat{T}}{\lambda}\right)\frac{\partial\hat{\Psi}}{\partial\hat{T}} \\ &\quad + \lambda^2\left(-\frac{\hat{\mu}}{\lambda}\right)\frac{\partial\hat{\Psi}}{\partial\hat{\mu}} \\ &= 2\lambda\left(\hat{\Psi} + \frac{Z}{2\pi}\ln\lambda + \frac{Z}{4\pi} + \frac{1}{2}\hat{T}\,\hat{s} + \frac{1}{2}\hat{\mu}\,\hat{\rho}\right).\end{aligned} \tag{3.25}$$

Since $\hat{\Psi} = \hat{u} - \hat{T}\,\hat{s} - \hat{\mu}\,\hat{\rho}$, we can express the minimization condition $\frac{\partial\Psi}{\partial\lambda} = 0$ in terms of the free energy as

$$\hat{u} = -\frac{Z}{4\pi} - \frac{Z}{2\pi}\ln\lambda + \frac{1}{2}\hat{\mu}\,\hat{\rho} + \frac{1}{2}\hat{T}\,\hat{s}. \tag{3.26}$$

If we impose also the condition (3.23) arising from the minimization with respect to the phase parameter q, we obtain the condition

$$\hat{u} = -\frac{Z}{4\pi} - \frac{Z}{2\pi}\ln\lambda + \frac{\hat{\mu}^2}{2\pi} + \frac{1}{2}\hat{T}\,\hat{s}. \tag{3.27}$$

Alternatively, we can express these conditions in terms of the thermodynamic quantities for the general condensate $\Delta(x)$ in (3.11). Without using the condition (3.24) arising from the q minimization, the λ minimization condition (3.26) can be written as

$$u = -\frac{Z\lambda^2}{4\pi} + \frac{1}{2}\mu\rho + \frac{1}{2}Ts + \frac{q}{2}\left(\rho - \frac{\mu}{\pi}\right). \tag{3.28}$$

After imposing the condition (3.24) arising from the q minimization, the last term vanishes and we obtain

$$u = -\frac{Z\lambda^2}{4\pi} + \frac{\mu^2}{2\pi} + \frac{1}{2}Ts. \tag{3.29}$$

These conditions must hold for any form of the condensate $\Delta(x)$, and will prove very useful in studying the phase diagram of both the NJL_2 and GN_2 models.

D. Transformation property of the consistency condition

The final technical ingredient before studying the thermodynamics is the effect of the transformation (3.1) on the consistency condition (2.16). Note that the consistency condition (2.16) must be satisfied also at finite T and μ, for the gap equation to hold. Thus, the energy trace involves the thermodynamical Fermi factor, as in (2.16). As with the grand potential, density, entropy, and free energy, it is useful to express the consistency condition in terms of the condensate $\hat{\Delta}(x)$ obtained by setting the scale $\lambda = 1$, and phase $q = 0$. All we need to know is the effect of the transformation (3.2) on $\mathcal{N}(E)$. From the form of (2.26) it is clear that

$$\mathcal{N}(E) = \frac{1}{\lambda^2}\hat{\mathcal{N}}\left(\frac{E-q}{\lambda}\right) \tag{3.30}$$

where

$$\hat{\mathcal{N}}(E) \equiv \frac{i}{4\sqrt{(E^2-1)(E-\hat{E}_2)(E-\hat{E}_3)}}. \tag{3.31}$$

Hence we can write the consistency condition as

$$\int \frac{dE}{2\pi}\,\frac{\hat{\mathcal{N}}(E)}{1 + e^{\hat{\beta}(E-\hat{\mu})}} = 0. \tag{3.32}$$

Note that this integral is finite, even at $T = 0$, and no renormalization is required. The effect of this condition is to express one of the four parameters λ, q, θ, and ν, in terms of the others, in a manner depending on T and μ.

IV. THERMODYNAMICS OF THE SPIRAL CONDENSATE

Before studying the general twisted kink crystal condensate, we investigate the thermodynamics of the special case of the spiral condensate:

$$\Delta(x) = \lambda e^{2iqx}. \tag{4.1}$$

For this condensate, $\hat{\Delta}(x) = 1$ (i.e., the vacuum fermion mass in our units) and so the thermodynamics is simply that of a constant condensate of unit magnitude. The fermion spectrum is now symmetric about 0, and so we can immediately write an expression for the corresponding grand potential $\hat{\Psi}$:

$$\hat{\Psi} = -\frac{1}{4\pi} - \frac{\hat{T}}{\pi}\int_1^\infty dE\,\frac{E}{\sqrt{E^2-1}} \times \ln((1 + e^{-\hat{\beta}(E-\hat{\mu})})(1 + e^{-\hat{\beta}(E+\hat{\mu})})). \tag{4.2}$$

The full grand potential Ψ for the spiral condensate (4.1) is then obtained using (3.16). Next we minimize the full grand potential Ψ with respect to q and λ.

A. Minimization with respect to the phase parameter q

At $T = 0$, we see from (4.2) that $\hat{\Psi} = -\frac{1}{4\pi}$, independent of $\hat{\mu}$, so that $\hat{\rho} = 0$. Therefore, the condition (3.23), arising from the minimization with respect to q, implies that $\hat{\mu} = 0$ at $T = 0$. In other words, $q = \mu$, so that the chemical potential lies at the center of the gap in the single-particle fermionic spectrum. With $q = \mu$, the spiral condensate (4.1) is the "chiral spiral" solution proposed in [15]. At nonzero temperature, the q minimization condition (3.23) can be written explicitly as

$$\begin{aligned}\hat{\mu} = \pi\hat{\rho} &= \pi\frac{\partial\hat{\Psi}}{\partial\hat{\mu}} \\ &= 2\sinh(\hat{\beta}\,\hat{\mu})\int_1^\infty dE\,\frac{E}{\sqrt{E^2-1}} \\ &\quad\times \frac{e^{\hat{\beta}E}}{(1 + e^{\hat{\beta}(E-\hat{\mu})})(1 + e^{\hat{\beta}(E+\hat{\mu})})}.\end{aligned} \tag{4.3}$$

At low temperatures, $T \ll 1$, the main contribution to the energy integrals in (4.3) comes from near the upper band edge $E = 1$. So we approximate the density of states as

$$\hat{\rho}(E) \approx \frac{1}{\sqrt{2}\sqrt{E-1}} \tag{4.4}$$

and (4.3) becomes

$$\hat{\mu} \approx \sqrt{2}\sinh(\hat{\beta}\,\hat{\mu}) \int_1^\infty dE \frac{1}{\sqrt{E-1}} e^{\hat{\beta}E} e^{-\hat{\beta}(E-\hat{\mu})} e^{-\hat{\beta}(E+\hat{\mu})}$$
$$= \sqrt{\frac{2\pi T}{\lambda}} e^{-\hat{\beta}} \sinh(\hat{\beta}\,\hat{\mu}). \quad (4.5)$$

This also requires $\hat{\mu} = 0$, leading again to the chiral spiral solution with $q = \mu$. Indeed, it is easy to verify numerically that the finite temperature equation (4.3) has a solution only at $\hat{\mu} = 0$, for all temperature T. Another argument in favor of $\mu = q$ at all temperatures is that instead of minimizing with respect to q, we can minimize with respect to $\hat{\mu}$. Since $\hat{\Psi}$ is symmetric under $\hat{\mu} \to -\hat{\mu}$, there must be a stationary point at $\hat{\mu} = 0$, i.e., $\mu = q$. That it is a minimum can easily be seen by looking at the sign of the 2nd derivative (Taylor expansion of the integrand). Other minima (which could only come in pairs) are ruled out numerically.

Thus, we conclude that the minimization of the grand potential with respect to the phase parameter q leads to $q = \mu$ for all temperature T, so μ always lies at the center of the gap. As should be clear from this discussion, this fact can be traced directly to the phase transformation symmetry in (3.1).

Another immediate consequence of $q = \mu$ is that the grand potential for the chiral spiral has a simple μ dependence. This follows because (3.23) with $\hat{\mu} = 0$ implies that $\hat{\Psi}$ is independent of the chemical potential μ. Indeed, when $\hat{\mu} = 0$, the grand potential (4.2) can then be written as

$$\hat{\Psi} = -\frac{1}{4\pi} - \frac{2\hat{T}}{\pi} \int_1^\infty dE \frac{E}{\sqrt{E^2-1}} \ln(1 + e^{-\hat{\beta}E}). \quad (4.6)$$

Then the general relation (3.16) implies that for the chiral spiral condensate the full grand potential is

$$\Psi = \frac{\lambda^2}{4\pi}(\ln\lambda^2 - 1) - \frac{2\lambda T}{\pi} \int_1^\infty dE \frac{E}{\sqrt{E^2-1}} \times \ln(1 + e^{-\hat{\beta}E}) - \frac{\mu^2}{2\pi}. \quad (4.7)$$

Thus, the grand potential for the chiral spiral has a simple μ dependence, and it is clear that $\rho = -\partial\Psi/\partial\mu = \mu/\pi$.

B. Minimization with respect to the scale parameter λ

From (4.7) it also follows that the scale parameter λ is determined only by T, independent of the chemical potential μ. Indeed, minimizing (4.7) with respect to λ, we obtain the equation for the thermal mass scale $\lambda(T)$:

$$0 = \lambda\frac{\ln\lambda}{\pi} - \frac{2T}{\pi} \int_1^\infty dE \frac{E}{\sqrt{E^2-1}} \ln(1 + e^{-\hat{\beta}E}) + \lambda\frac{2}{\pi} \int_1^\infty dE \frac{E^2}{\sqrt{E^2-1}} \frac{1}{1 + e^{\hat{\beta}E}}. \quad (4.8)$$

It is a simple exercise to show that this is equivalent to the general λ minimization condition (3.29), expressed in terms of the entropy and the free energy. Note that this equation does not involve the chemical potential μ, so the thermal mass scale $\lambda(T)$ must be independent of μ.

At $T = 0$, (4.8) reduces to $\lambda\ln\lambda = 0$, which implies that $\lambda(T = 0) = 1$, and the grand potential is simply

$$\Psi_{\min}^{T=0} = -\frac{1}{4\pi} - \frac{\mu^2}{2\pi}. \quad (4.9)$$

For small but nonzero temperature, the scale parameter λ receives an exponentially small finite T correction, found by approximating the energy integrals in (4.8)

$$\lambda(T) \sim 1 - \sqrt{2\pi T} e^{-1/T}, \qquad T \ll 1. \quad (4.10)$$

Applying the same approximation to the minimized grand potential in (4.7) we find the leading small T correction to the grand potential:

$$\Psi_{\min}^{T\ll 1} \sim \frac{\lambda^2}{4\pi}(\ln\lambda^2 - 1) - \sqrt{\frac{2T^3}{\pi}} e^{-1/T} - \frac{\mu^2}{2\pi}$$
$$\sim -\frac{1}{4\pi} - \frac{\mu^2}{2\pi} - \sqrt{\frac{2T^3}{\pi}} e^{-1/T}. \quad (4.11)$$

For general T, the temperature dependent mass scale $\lambda(T)$ can be obtained numerically from (4.8). The scale $\lambda(T)$ decreases monotonically from the value $\lambda = 1$ at $T = 0$, and vanishes at a critical temperature

$$T_c = \frac{e^\gamma}{\pi} \approx 0.566\,933. \quad (4.12)$$

At this temperature, $T = T_c$, the system undergoes a phase transition to a massless phase. Interestingly, this phase transition is independent of the chemical potential μ, as follows from the fact that $\lambda(T)$ is independent of μ. We can trace this fact directly to the simple form (4.7) of the grand potential for the chiral spiral condensate, after minimization with respect to the scale parameter q.

Just below T_c the dependence of λ on T is nonanalytic, as can be seen from the following argument. After integrating by parts the second integral in (4.8), and expanding the Fermi factor we obtain

$$0 = \ln\lambda + 2\sum_{n=1}^\infty (-1)^{n+1} \int_1^\infty dE \frac{1}{\sqrt{E^2-1}} e^{-n\hat{\beta}E}$$
$$= \ln\lambda + 2\sum_{n=1}^\infty (-1)^{n+1} K_0(n\hat{\beta}) \quad (4.13)$$

where $K_0(x)$ is the modified Bessel function. To obtain the critical exponents near the phase transition, we analyze this equation near small values of λ. Since $\hat{\beta} = \lambda/T$ we expand the Bessel functions around zero:

$$0 = \ln\lambda + 2\sum_{n=1}^{\infty}(-1)^{n+1}\Big[-\ln\Big(\frac{n\lambda}{2T}\Big) - \gamma - \frac{n^2\lambda^2}{4T^2}\Big(\ln\Big(\frac{n\lambda}{2T}\Big) + \gamma - 1\Big)\Big]. \tag{4.14}$$

Here γ is Euler's constant. The n sums can be evaluated in terms of the Riemann zeta function, leading to

$$0 = \ln(T\pi) - \gamma - \frac{14\zeta'(-2)\lambda^2}{4T^2}. \tag{4.15}$$

In particular, at the phase transition where $\lambda = 0$, the critical temperature is found to be $T_c = e^{\gamma}/\pi$, and to the leading order in $(T_c - T)$, for $T < T_c$:

$$\lambda(T) = \sqrt{\frac{2T_c}{-7\zeta'(-2)}}\sqrt{T_c - T} + \ldots \approx 3.06\sqrt{T_c(T_c - T)} + \ldots \tag{4.16}$$

Thus, for the spiral condensate (4.1), the thermodynamic phase diagram is given in Fig. 5, showing the phase transition at $T = T_c$, independent of μ. After minimizing the grand potential we learn that in the region $T < T_c$, the pitch angle q of the spiral condensate is directly proportional to the chemical potential, $q = \mu$, independent of T, while the amplitude $\lambda(T)$ is just a function of temperature (vanishing at T_c), independent of μ.

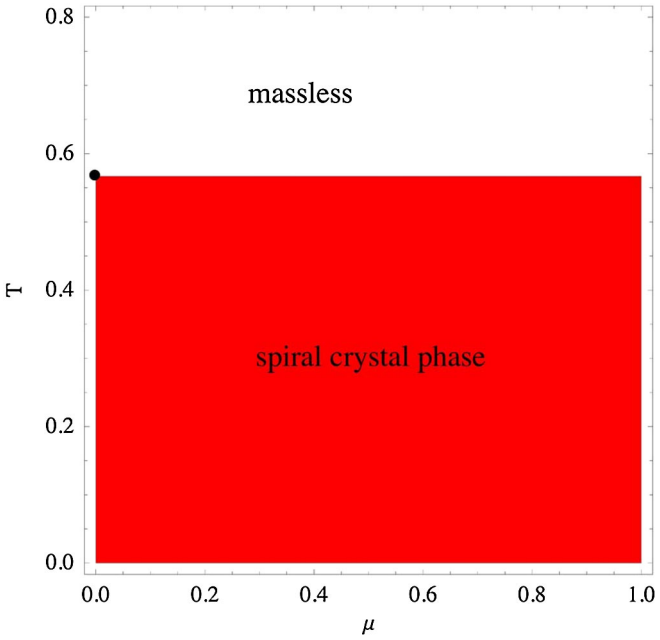

FIG. 5 (color online). The phase diagram of the NJL_2 model. The tricritical point is marked at $\mu_{tc} = 0$ and $T_{tc} = e^{\gamma}/\pi \approx 0.5669$. Below T_c the condensate has the form of the spiral condensate (4.1), with $q = \mu$.

V. THERMODYNAMICS OF THE TWISTED CRYSTAL CONDENSATE

In this section we develop results for the thermodynamics of the NJL_2 model with the twisted kink crystal condensate, that is the general solution of the inhomogeneous gap equation. Recall that the twisted kink crystal condensate (2.20) is characterized by 4 parameters: the scale parameter λ, the phase parameter q, an angular parameter θ, and the elliptic parameter ν. We first consider the situation analytically at $T = 0$, then at nonzero T.

A. Twisted kink crystal at $T = 0$

At $T = 0$ there are some significant simplifications. First of all, the Fermi factor becomes a step function that acts as a cutoff of the energy integrals. Thus, in the consistency condition (3.32), we use

$$\frac{1}{1 + e^{\hat{\beta}(E-\hat{\mu})}} \to \Theta(\hat{\mu} - E). \tag{5.1}$$

If we assume that $\hat{\mu}$ is in the upper gap, then both the lower continuum and the bound band are completely filled. Thus the consistency condition (3.32) reads (for details, see [14])

$$0 = \int_{-\infty}^{-1} dE\mathcal{N}(E) + \int_{E_2}^{E_3} dE\mathcal{N}(E) = \frac{1}{2A}\Big(\frac{\theta}{4} - \mathbf{K}'\Big). \tag{5.2}$$

Therefore, the consistency condition forces $\theta = 4\mathbf{K}'$, which is precisely the spiral condensate case. In this limit, the band shrinks and joins the negative energy continuum, leaving just the single-gap spectrum of the spiral condensate. Then the q minimization leads to $q = \mu$ as described in the previous section, and we find the preferred condensate to be the chiral spiral. Similarly, if we assume that $\hat{\mu}$ is in the lower gap, then we get $\theta = 0$, that is also the spiral condensate limit; in this limit the bound band joins to the positive energy continuum. Once again, minimization with respect to the phase parameter q leads to $q = \mu$, so the condensate is the chiral spiral.

The only other possibility is $\hat{\mu}$ lying inside the bound band. In this case the consistency condition (2.16) leads to an expression for the Fermi energy:

$$\hat{E}_F = \hat{E}_F(\theta, \nu) = \mathrm{nc}(i\theta/2; \nu). \tag{5.3}$$

On the other hand, at $T = 0$, this Fermi energy is simply the chemical potential. Minimization with respect to the phase parameter q leads to the relation $\hat{\mu} = \pi\hat{\rho}$. We can evaluate the density obtained by filling up to the Fermi energy $\hat{E}_F(\theta, \mu)$:

$$\hat{\rho} = \hat{\rho}(\theta, \nu) = \frac{1}{\pi}\frac{1}{\mathrm{cn}(i\theta/2; \nu)}\Big(\frac{\mathrm{cn}(i\theta/2; \nu) - \mathrm{dn}(i\theta/2; \nu)}{\mathrm{cn}(i\theta/2; \nu) + \mathrm{dn}(i\theta/2; \nu)}\Big). \tag{5.4}$$

The simultaneous solution of these two conditions, namely

$\hat{E}_F = \pi\hat{\rho}$, has the unique solution $\theta = 2\mathbf{K}'$, for all ν, as can be seen from Fig. 6. Evaluating the free energy for this solution we obtain the following function of the remaining parameters λ and ν:

$$\mathcal{E} = \mathcal{E}(\lambda, \nu) = \frac{2\lambda^2}{\pi(1+\sqrt{\nu})^2}\left[\frac{\nu}{2} + \left(1 - \frac{\mathbf{E}(\nu)}{\mathbf{K}(\nu)}\right)\left(\ln\left(\frac{2\lambda}{1+\sqrt{\nu}}\right) - 1\right)\right] + \frac{\mu^2}{2\pi}. \tag{5.5}$$

Minimizing $\mathcal{E}(\lambda, \nu)$ with respect to ν, we find that we are forced to $\nu = 1$, which means

$$\mathcal{E}(\lambda, \nu = 1) = \frac{\lambda^2}{4\pi}(\ln\lambda^2 - 1) + \frac{\mu^2}{2\pi} \tag{5.6}$$

from which we recognize the $T = 0$ grand potential (4.7) of the chiral spiral solution. Thus, once again, the minimization forces us to the chiral spiral condensate solution, at $T = 0$.

B. Twisted kink crystal at $0 < T \ll 1$

The minimization of the grand potential at $T = 0$ shows that the preferred twisted kink crystal configuration is the chiral spiral, with the chemical potential sitting in the middle of the gap (i.e., $\hat{\mu} = (\mu - q)/\lambda = 0$). For this solution, the angular parameter θ takes the values 0 or $4\mathbf{K}'$. We will consider the latter case (a similar argument applies for the other choice). Now consider the stability of this chiral spiral for T nonzero but small. If we change T slightly away from 0, then the consistency condition that sets the angular parameter $\theta = 4\mathbf{K}'$, will also change slightly, and the preferred value of θ will shift away from $4\mathbf{K}'$. We write $\theta = 4\mathbf{K}' - 4\epsilon$, where $\epsilon \ll \hat{T} \ll 1$. This changes the single-particle spectrum by producing a very narrow band very close to the lower band edge $\hat{E}_1 = -1$.

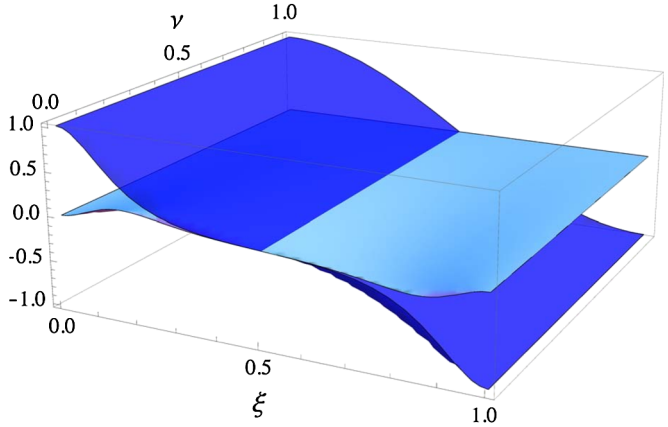

FIG. 6 (color online). Plot of $\pi\hat{\rho}(\xi, \nu)$ (light blue surface) and $\hat{E}_F(\xi, \nu)$ (darker blue surface), as functions of ν and ξ, where $\theta \equiv 4\mathbf{K}'\xi$. The surfaces intersect at $\xi = 1/2$, which means $\theta = 2\mathbf{K}'$.

With $\theta = 4\mathbf{K}' - 4\epsilon$, the band edges (3.5) and the averaged amplitude (2.28) take the form

$$\begin{aligned}\hat{E}_2(\theta, \nu) &\approx -1 + 2\nu\epsilon^2 + \ldots \\ \hat{E}_3(\theta, \nu) &\approx -1 + 2\epsilon^2 + \ldots \\ Z(\theta, \nu) &\approx 1 - h(\nu)\epsilon^2 + \ldots\end{aligned} \tag{5.7}$$

where $h(\nu) = 2\nu - 2 + 4\mathbf{E}(\nu)/\mathbf{K}(\nu)$. We now calculate the small T correction to the grand potential $\hat{\Psi}$ for this configuration. As usual, we split the grand potential into zero temperature and finite temperature parts. For small T, we use the fact that $\ln(1 + e^{-|\hat{\beta}(E-\hat{\mu})|}) \approx e^{-|\hat{\beta}(E-\hat{\mu})|} \approx e^{-\hat{\beta}|E|}$ (recall that $\hat{\mu} = 0$ for $T = 0$)

$$\begin{aligned}\hat{\Psi} &\approx \int_{-\infty}^{-1} dE\hat{\rho}(E)(E - \hat{\mu}) + \int_{E_2}^{E_3} dE\hat{\rho}(E)(E - \hat{\mu}) \\ &\quad - T\left(\int_{-\infty}^{-1} dE\hat{\rho}(E)e^{\hat{\beta}E} + \int_{1}^{\infty} dE\hat{\rho}(E)e^{-\hat{\beta}E} + \int_{E_2}^{E_3} dE\bar{\rho}(E)e^{\hat{\beta}E}\right) \\ &= \langle\hat{\Psi}\rangle_{T=0} - Te^{-\hat{\beta}}\left(\int_0^{\infty} dx\hat{\rho}(-x-1)e^{-\hat{\beta}x} + \int_0^{\infty} dx\hat{\rho}(x+1)e^{-\hat{\beta}x} + \int_{2\nu\epsilon^2}^{2\epsilon^2} dx\hat{\rho}(x-1)e^{\hat{\beta}x}\right).\end{aligned} \tag{5.8}$$

In the small T limit, the continuum integrals are dominated by the region $x \approx 0$ (i.e., near the band edges). The spectral function around the band edges has the behavior

$$\int_0^{\infty} dx\hat{\rho}(-x-1)e^{-\hat{\beta}x} = \sqrt{\frac{T}{2\pi}} - \epsilon\frac{1}{\mathbf{K}(\sqrt{\nu})} \tag{5.9}$$

$$\int_0^{\infty} dx\hat{\rho}(x+1)e^{-\hat{\beta}x} \approx \sqrt{\frac{T}{2\pi}} + O(\epsilon^2). \tag{5.10}$$

Note that the lower continuum leads to an $O(\epsilon)$ correction, while the upper continuum leads to an $O(\epsilon^2)$ correction. The band integral also leads to an $O(\epsilon)$ correction. This can be seen by changing the integration variable $x \to \epsilon^2 x$:

$$\begin{aligned}\int_{2\nu\epsilon^2}^{2\epsilon^2} dE\hat{\rho}(x-1)e^{\hat{\beta}x} &= \epsilon\int_{2\nu}^{2} dx e^{\hat{\beta}x\epsilon^2}\frac{-x-(1+\nu)-h(\nu)/2}{\pi\sqrt{x(x-2\nu)(2-x)}} \\ &\approx \epsilon\int_{2\nu}^{2} dx\frac{2-x-2\mathbf{E}(\nu)/\mathbf{K}(\nu)}{\pi\sqrt{x(x-2\nu)(2-x)}} \\ &\equiv \epsilon L(\nu).\end{aligned} \tag{5.11}$$

An important observation is that this function $L(\nu) < 0$ for all $\nu \in [0, 1]$.

Finally, we use the general transformation of the grand potential (3.16) to deduce the grand potential for the twisted kink crystal. Since after minimization, $\hat{\psi}_{T=0} = -1/(4\pi)$, the small T correction to λ does not contribute to the full grand potential Ψ [as in (4.11)], and the full

grand potential is found to be

$$\Psi \approx \left(-\frac{1}{4\pi}-\frac{\mu^2}{2\pi}-\sqrt{\frac{2T^3}{\pi}}e^{-1/T}\right)+\epsilon\left(\frac{1}{\mathbf{K}(\sqrt{\nu})}-L(\nu)\right)Te^{-1/T}+\ldots \tag{5.12}$$

The first term in parentheses is just the low T grand potential for the chiral spiral, as in (4.11). Since $L(\nu)$ is always negative, and $\mathbf{K}(\sqrt{\nu})$ is always positive, we see that the system is unstable with respect to the opening of a gap near the lower continuum edge. In other words, at small T the minimization of the grand potential reduces the general twisted kink crystal condensate to the chiral spiral condensate, just as at $T=0$.

C. Numerical results for the thermodynamics of the twisted kink crystal condensate

The previous two sections have shown that at $T=0$ and for small T, the chiral spiral condensate is the thermodynamically preferred form of the more general twisted kink crystal condensate. We have also checked this conclusion numerically at various locations on the phase diagram, and we find that throughout the phase diagram the chiral spiral is the thermodynamically preferred limit of the general twisted kink crystal solution of the inhomogeneous gap equation.

VI. THERMODYNAMICS OF THE REAL KINK CRYSTAL AND THE GN_2 MODEL

The phase diagram of the GN_2 model, which has just a *discrete* chiral symmetry instead of the *continuous* chiral symmetry of the NJL_2 model, is by now well understood [16,34]. But we revisit it here briefly, with a new perspective. The analysis of this paper shows that the key to understanding the phase diagram of the NJL_2 model is the behavior (3.16) of the renormalized grand potential under the rescaling and shifting transformation (3.1). But in the GN_2 model there is no pseudoscalar interaction, so the condensate is real. Thus, there is no symmetry corresponding to a phase rotation of the condensate. In other words, $q\equiv 0$. The angular parameter θ in the solution (2.20) of the inhomogeneous gap equation is also zero, as the condensate cannot wind by an arbitrary phase as it goes through one period. Furthermore, there is no need to impose any consistency condition on the solution of the gap equation: since the pseudoscalar condensate Π is identically zero, there is no condition arising from its variation, which means that the off diagonal terms in (2.11) play no role. Thus, the general solution (2.20) of the inhomogeneous gap equation simplifies to the real kink crystal solution in (2.32), which depends on just two parameters, the scale λ and the elliptic parameter ν. Concerning the grand potential, the key formula is now (3.16), with q set to 0:

$$\Psi_{\rm ren}[\lambda\hat{\Delta}(\lambda x);T,\mu]=\lambda^2\left(\hat{\Psi}_{\rm ren}[\hat{\Delta}(x);T/\lambda,\mu/\lambda]+\frac{Z}{2\pi}\ln\lambda\right). \tag{6.1}$$

The last term reflects the anomalous behavior of the grand potential under the rescaling of the condensate by λ.

A. Real kink crystal at $T=0$

From previous work [16], we know explicit expressions for the thermodynamical quantities at $T=0$ as functions of the elliptic parameter ν. For $\lambda=1$, the density is

$$\hat{\rho}=\frac{1}{2\mathbf{K}(\tilde{\nu})},\qquad \tilde{\nu}\equiv\frac{4\sqrt{\nu}}{(1+\sqrt{\nu})^2}. \tag{6.2}$$

The free energy is

$$\hat{\mathcal{E}}=\frac{Z(\tilde{\nu})}{4\pi}(\ln\tilde{\nu}-1)+\frac{1}{2\pi}\frac{\mathbf{E}(\tilde{\nu})}{\mathbf{K}(\tilde{\nu})} \tag{6.3}$$

where

$$Z(\tilde{\nu})=2\left(1-\frac{\tilde{\nu}}{2}-\frac{\mathbf{E}(\tilde{\nu})}{\mathbf{K}(\tilde{\nu})}\right) \tag{6.4}$$

which is just $Z(\theta,\nu)$ in (2.28), evaluated at $\theta=2\mathbf{K}'(\nu)$.

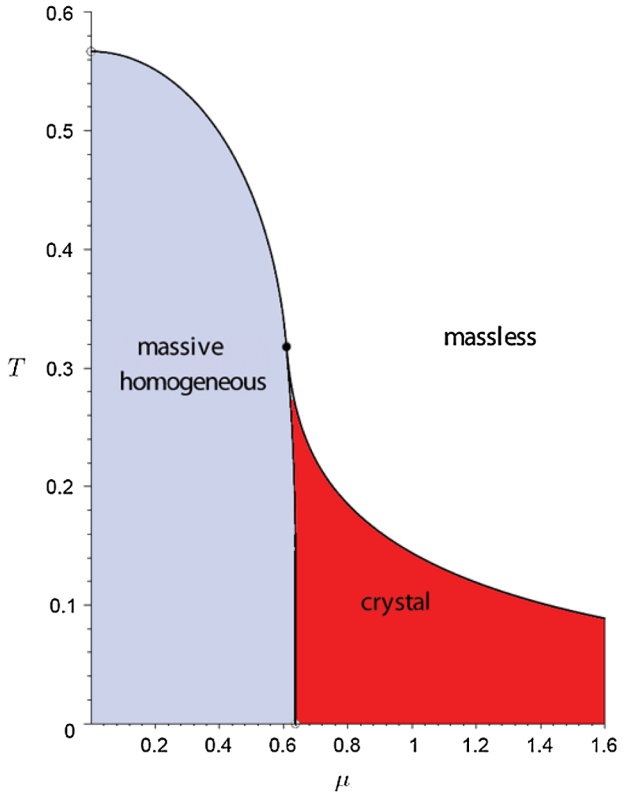

FIG. 7 (color online). Phase diagram of the GN_2 model. The tricritical point is at $\mu_{\rm tc}=0.608$ and $T_{\rm tc}=0.318$. In the region of $\mu>2/\pi$, the massless and massive phases are separated by a crystalline phase.

The function $\mathbf{E}(\tilde{\nu})$ is the complete elliptic integral of the second kind [33]. Thus we can write the $T = 0$ grand potential as

$$\Psi = \mathcal{E} - \mu\rho = \lambda^2(f_1(\tilde{\nu}) + f_2(\tilde{\nu})\ln\lambda) - \mu\lambda f_3(\tilde{\nu}) \tag{6.5}$$

where

$$f_1(\tilde{\nu}) \equiv \frac{Z(\tilde{\nu})}{4\pi}(\ln\tilde{\nu} - 1) + \frac{1}{2\pi}\frac{\mathbf{E}(\tilde{\nu})}{\mathbf{K}(\tilde{\nu})} \tag{6.6}$$

$$f_2(\tilde{\nu}) \equiv \frac{Z(\tilde{\nu})}{2\pi} \tag{6.7}$$

$$f_3(\tilde{\nu}) \equiv \frac{1}{2\mathbf{K}(\tilde{\nu})}. \tag{6.8}$$

Minimizing Ψ with respect to λ and $\tilde{\nu}$ leads to two equations:

$$\begin{aligned}\frac{\partial\Psi}{\partial\lambda} &= 2\lambda\left(f_1 + \frac{1}{2}f_2 + f_2\ln\lambda\right) - \mu f_3 = 0\\ \frac{\partial\Psi}{\partial\tilde{\nu}} &= \lambda\{\lambda(f_1' + f_2'\ln\lambda) - \mu f_3'\} = 0.\end{aligned} \tag{6.9}$$

Simultaneous solution of these conditions leads to a complicated-looking expression for $\ln\lambda$, that actually simplifies dramatically:

$$\ln\lambda = \frac{f_3 f_1' - 2f_3'(f_1 + f_2/2)}{2f_2 f_3' - f_3 f_2'} = -\frac{1}{2}\ln\tilde{\nu}. \tag{6.10}$$

In showing this remarkable reduction we use the property

$$\frac{\partial Z}{\partial\tilde{\nu}} = \frac{(Z - \tilde{\nu})^2}{4\tilde{\nu}(1 - \tilde{\nu})}. \tag{6.11}$$

Inserting this result for λ back into the minimization conditions (6.9) we find the minimized values at $T = 0$:

$$\mu(\tilde{\nu}) = \frac{2\mathbf{E}(\tilde{\nu})}{\pi\sqrt{\tilde{\nu}}} \tag{6.12}$$

$$\lambda(\tilde{\nu}) = \frac{1}{\sqrt{\tilde{\nu}}}. \tag{6.13}$$

The critical value of chemical potential, $\mu_c = \frac{2}{\pi}$, corresponding to the baryon mass [9,10,18], is obtained at $\tilde{\nu} = 1$, in agreement with known results [16].

B. Real kink crystal at $T \ll 1$

At nonzero temperature, the minimization with respect to λ and $\tilde{\nu}$ leads to T dependent expressions for the chemical potential and the scale factor λ, as functions of the elliptic parameter $\tilde{\nu}$, generalizing the $T = 0$ expressions (6.12) and (6.13). This can be done numerically, as in [16], but here we find analytic expressions valid in the small T limit. First, we note that the $T = 0$ chemical potential in (6.12) lies in the upper gap (see Fig. 8):

$$E_3(\tilde{\nu}) = \lambda(\tilde{\nu})\sqrt{1 - \tilde{\nu}} \le \mu(\tilde{\nu}) \le E_4(\tilde{\nu}) = \lambda(\tilde{\nu}). \tag{6.14}$$

Since μ is in the gap, at small T there is an exponentially small factor in the corrections to thermodynamic quantities going like

$$\exp[-|\mu - \text{nearest band edge}|/T]. \tag{6.15}$$

Furthermore, for all $\tilde{\nu}$, μ is closer to E_4 than to E_3. Thus, we can write as a leading approximation

$$\Psi = -T\int dE\rho(E)\ln(1 + e^{-\beta(E-\mu)}) \tag{6.16}$$

$$= \Psi_{T=0} - T\int dE\rho(E)\ln(1 + e^{-\beta|E-\mu|}) \tag{6.17}$$

$$\sim \Psi_{T=0} - Te^{-\beta(E_4-\mu)}\int_{E_4}^{\infty} dE\rho(E)e^{-\beta(E-E_4)}. \tag{6.18}$$

We expand the spectral function in the vicinity of the nearer band edge, E_4:

$$\rho(E) = \frac{2E^2 - (E_3^2 + E_4^2) + \lambda^2 Z}{2\pi\sqrt{(E^2 - E_3^2)(E^2 - E_4^2)}} \tag{6.19}$$

$$\sim \frac{1}{2\pi}\frac{E_4^2 - E_3^2 + \lambda^2 Z}{\sqrt{2E_4(E_4^2 - E_3^2)}}\frac{1}{\sqrt{E - E_4}} + O(\sqrt{E - E_4}). \tag{6.20}$$

Thus,

$$\Psi \sim \Psi_{T=0} - T^{3/2}\sqrt{\frac{\lambda}{2\pi}}f_4(\tilde{\nu})e^{-\beta(E_4-\mu)} \tag{6.21}$$

where

$$f_4(\tilde{\nu}) = \frac{1}{\sqrt{\tilde{\nu}}}\left(1 - \frac{\mathbf{E}(\tilde{\nu})}{\mathbf{K}(\tilde{\nu})}\right). \tag{6.22}$$

We now minimize Ψ with respect to λ and $\tilde{\nu}$, keeping the leading small T corrections to the $T = 0$ results of the

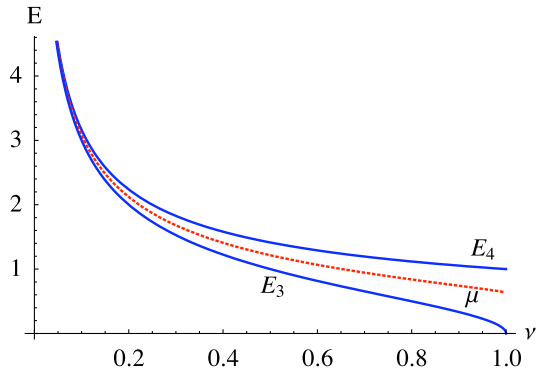

FIG. 8 (color online). Plot of the chemical potential (center line), and the band edge energies, as a function of the elliptic parameter $\tilde{\nu}$. Note that $\mu(\tilde{\nu})$ lies in the gap for all $\tilde{\nu}$, and moreover, it is slightly closer to the upper band edge, E_4, than to the lower band edge, E_3.

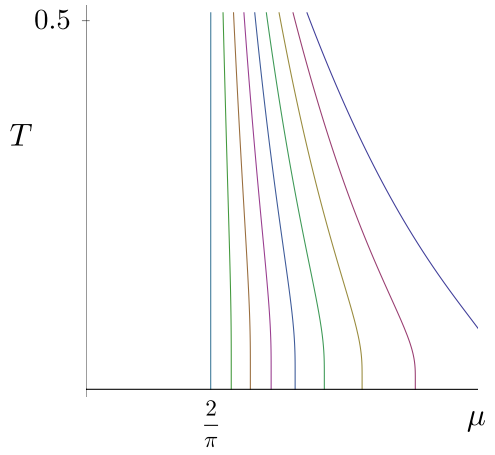

FIG. 9 (color online). Plots of the chemical potential, as a function of T, for various values of the elliptic parameter $\tilde{\nu}$, keeping just the leading small T behavior, as in (6.24). This plot is in remarkable agreement with the numerical results shown in Fig. 7.

previous section. We find, after some straightforward algebra,

$$\mu(\tilde{\nu},T) \sim \frac{2\mathbf{E}(\tilde{\nu})}{\pi\sqrt{\tilde{\nu}}} - \sqrt{\frac{2T}{\pi}}\frac{(1-\tilde{\nu})\mathbf{K}(\tilde{\nu})}{\tilde{\nu}^{3/4}} \times \exp\left[-\beta\left(\frac{1}{\sqrt{\tilde{\nu}}}\left(1-\frac{2\mathbf{E}(\tilde{\nu})}{\pi}\right)\right)\right] \tag{6.23}$$

$$\lambda(\tilde{\nu},T) \sim \frac{1}{\sqrt{\tilde{\nu}}} - \sqrt{\frac{\pi T}{2}}\frac{1}{\tilde{\nu}^{3/4}}\exp\left[-\beta\left(\frac{1}{\sqrt{\tilde{\nu}}}\left(1-\frac{2\mathbf{E}(\tilde{\nu})}{\pi}\right)\right)\right]. \tag{6.24}$$

These small T corrections are plotted in Fig. 9, and are in very good agreement with the numerical results found in [16], and plotted in Fig. 7. Already these corrections indicate the existence of a crystalline phase in which the condensate scale λ and the period (set by the elliptic parameter ν) are dependent on *both* T and μ. This is in contrast to the phase diagram of the NJL_2 model, shown in Fig. 5, where the phase transition line is only a function of T, and the scale parameter λ is independent of the chemical potential μ. With this perspective we can trace this fundamental difference in the phase diagrams directly to the fundamental difference between the discrete and continuous chiral symmetry of the two models.

VII. GINZBURG-LANDAU ANALYSIS

We complete our analysis of the phase diagram of the NJL_2 and GN_2 models by analyzing another region of the phase diagram, using the Ginzburg-Landau expansion of the grand potential Ψ. In the previous sections we obtained analytic results at and near $T=0$, but the Ginzburg-Landau approach permits a certain degree of analytic information about another region of the phase diagram, in the vicinity of the tricritical point. Expanding in powers of the condensate and its derivatives, the renormalized grand potential density may be expressed as

$$\begin{aligned}\Psi_{\mathrm{GL}} = {} & \alpha_0 + \alpha_2|\Delta|^2 + \alpha_3\,\mathrm{Im}(\Delta\Delta'^*) + \alpha_4(|\Delta|^4 + |\Delta'|^2) \\ & + \alpha_5\,\mathrm{Im}((\Delta'' - 3|\Delta|^2\Delta)\Delta'^*) + \alpha_6(2|\Delta|^6 \\ & + 8|\Delta|^2|\Delta'|^2 + 2\,\mathrm{Re}\Delta'^2\Delta^{*2} + |\Delta''|^2) + \ldots \end{aligned} \tag{7.1}$$

The coefficients $\alpha_n(T,\mu)$ are the following functions of T and μ [16]:

$$\begin{aligned}\alpha_0 &= -\frac{\pi T^2}{6} - \frac{\mu^2}{2\pi} \\ \alpha_2 &= \frac{1}{2\pi}\left[\ln(4\pi T) + \mathrm{Re}\,\psi\left(\frac{1}{2} + i\frac{\beta\mu}{2\pi}\right)\right] \\ \alpha_3 &= -\frac{1}{2^3\pi^2 T}\,\mathrm{Im}\,\psi^{(1)}\left(\frac{1}{2} + i\frac{\beta\mu}{2\pi}\right) \\ \alpha_4 &= -\frac{1}{2^6\pi^3 T^2}\,\mathrm{Re}\,\psi^{(2)}\left(\frac{1}{2} + i\frac{\beta\mu}{2\pi}\right) \\ \alpha_5 &= -\frac{1}{2^8\pi^4 3T^3}\,\mathrm{Im}\,\psi^{(3)}\left(\frac{1}{2} + i\frac{\beta\mu}{2\pi}\right) \\ \alpha_6 &= \frac{1}{2^{12}\pi^5 3T^4}\,\mathrm{Re}\,\psi^{(4)}\left(\frac{1}{2} + i\frac{\beta\mu}{2\pi}\right). \end{aligned} \tag{7.2}$$

Here $\psi^{(n)}(x)$ is the nth derivative of the digamma function $\psi(x) \equiv \Gamma'(x)/\Gamma(x)$.

Keeping terms up to a certain order in this expansion, and inserting into the gap equation (2.9), we obtain an equation (the Ginzburg-Landau equation) for the condensate Δ. Remarkably, for the NJL_2 and GN_2 models, this hierarchy of equations can be solved to all orders [14,26,27]. If we expand up to α_2, then the Ginzburg-Landau (GL) equation is simply $\Delta = 0$, so we learn nothing about the phase diagram. To this order the system appears to be just a free massless Fermi gas. If we expand Ψ up to α_3, then the GL equation reads

$$\Delta' - i\frac{\alpha_2}{\alpha_3}\Delta = 0 \Rightarrow \Delta = \lambda\exp\left[i\frac{\alpha_2}{\alpha_3}x\right]. \tag{7.3}$$

This has the form of the spiral condensate studied in Sec. II B. This spiral condensate has constant magnitude, $|\Delta|^2 = \lambda^2$, and also $\frac{1}{2i}(\Delta\Delta^{*\prime} - \Delta^*\Delta') = -\frac{\alpha_2}{\alpha_3}\lambda^2$, so that when we evaluate the grand potential on this solution, we find

$$\Psi_{\mathrm{GL}} = \alpha_0. \tag{7.4}$$

So the grand potential is independent of λ, and this is again no different from a free massless phase. If we expand up to α_4, then the GL equation is the NLSE equation:

$$(\Delta'' - 2|\Delta|^2\Delta) - i\frac{\alpha_3}{\alpha_4}\Delta' - \frac{\alpha_2}{\alpha_4}\Delta = 0. \tag{7.5}$$

The general bounded solution of this equation is the twisted kink crystal described in Sec. II A.

The general pattern is the following: to order α_k, the GL equation is a differential equation of order $(k-2)$, and the general solution corresponds to a finite-gap Dirac problem with $(k-2)$ gaps, or $(k-1)$ bands (including the positive and negative continuum bands). For example, the α_2 equation led to $\Delta = 0$, which is the free system with no gaps. The α_3 equation leads to $\Delta = \lambda \exp[i\frac{\alpha_2}{\alpha_3}x]$, which has precisely one gap. The α_4 equation, the NLSE (2.15), has as its general solution a system with two gaps, as shown in the first plot of Fig. 2. In general the solution with $(k-2)$ gaps requires $2(k-2)$ parameters for the solution, and these parameters can be thought of as labelling the band edges. Let us write

$$\Psi_{\rm GL} = \alpha_0(T,\mu) + \sum_{l=2}^{\infty} \alpha_l(T,\mu) J_l[\Delta, \Delta', \Delta'', \ldots] \quad (7.6)$$

where $J_l[\Delta, \Delta', \Delta'', \ldots]$ represents the nonlinear combinations of the condensate $\Delta(x)$ and its derivative appearing in the expansion (7.1). Then the GL equation to order k is

$$\sum_{l=2}^{k} \alpha_l(T,\mu) \frac{\delta J_l[\Delta, \Delta', \Delta'', \ldots]}{\delta \Delta^*(x)} = 0. \quad (7.7)$$

These equations define the Ablowitz-Kaup-Newell-Segur (AKNS) hierarchy, and (7.7) is also known as the Novikov equation. Formal expressions exist for their solution in terms of multidimensional theta functions [26,27], although these are cumbersome to work with beyond the twisted kink crystal solution. The remarkable integrability properties of the AKNS hierarchy implies that the solution to the NLSE satisfies the Novikov equations to all orders, with suitable choices of parameters, as shown also in [14].

A. Ginzburg-Landau expansion for the GN_2 model

It is instructive to see how successive orders of the Ginzburg-Landau expansion reveal more and more about the exact phase diagram. In the GN_2 system, the condensate is real, and we write it as $\Delta = \phi$, and all odd-index terms of the Ginzburg-Landau expansion vanish. The Dirac spectrum is now symmetric about 0, and so the band edges of the finite-gap solutions come in $\pm$ pairs, as in the 2-gap case depicted in the third plot of Fig. 2. Therefore, we only need half as many parameters at a given order to describe the solution. The grand potential density simplifies to

$$\begin{aligned}\Psi_{\rm GL} &= \alpha_0 + \alpha_2\phi^2 + \alpha_4(\phi^4 + \phi'^2 - \tfrac{1}{3}(\phi^2)'') \\ &\quad + \alpha_6(2\phi^6 + 10\phi^2\phi'^2 + \phi''^2 - (\phi^4 + (\phi')^2 \\ &\quad - \tfrac{1}{5}(\phi^2)'')'') + \ldots \end{aligned} \quad (7.8)$$

The tricritical point is defined as the point where the first two nontrivial coefficients, $\alpha_2(T,\mu)$ and $\alpha_4(T,\mu)$ vanish:

$$\begin{aligned}&\alpha_2(T,\mu) = \alpha_4(T,\mu) = 0 \Rightarrow T_{\rm tc} = 0.318\,329, \\ &\qquad \mu_{\rm tc} = 0.608\,221 \end{aligned} \quad (7.9)$$

1. Ginzburg-Landau expansion to $O(\alpha_4)$ for the GN_2 model

As mentioned above, the expansion to $O(\alpha_2)$ yields no information. The next nontrivial order, to $O(\alpha_4)$, leads to the following GL equation, which is a special case of the NLSE (7.5)

$$\phi'' - 2\phi^3 - \frac{\alpha_2}{\alpha_4}\phi = 0. \quad (7.10)$$

The general solution can be written as

$$\phi = \lambda\sqrt{\nu}\,\mathrm{sn}(\lambda x;\nu) \Leftrightarrow \phi'' - 2\phi^3 + (1+\nu)\lambda^2\phi = 0 \quad (7.11)$$

with the identification of the scale parameter λ as

$$\lambda^2 = \left(-\frac{\alpha_2}{\alpha_4}\right)\left(\frac{1}{1+\nu}\right). \quad (7.12)$$

Notice that in the GL approach, we get explicit expressions for the dependence of the solution's parameters in terms of T and μ. An important comment is that since $\frac{1}{1+\nu} \geq 0$, this expression tells us that this inhomogeneous solution only makes sense in regions of the (T,μ) plane where $(-\frac{\alpha_2}{\alpha_4}) \geq 0$. Using the following identities satisfied by the solution in (7.11)

$$(\phi')^2 = \phi^4 - (1+\nu)\lambda^2\phi^2 + \nu\lambda^4 \quad (7.13)$$

$$(\phi^2)'' = 6\phi^4 - 4(1+\nu)\lambda^2\phi^2 + 2\nu\lambda^4 \quad (7.14)$$

we can write the grand potential density to this order as

$$\begin{aligned}\Psi_{\rm GL} &= \alpha_0 + \alpha_2\phi^2 + \alpha_4\left(\frac{1}{3}(1+\nu)\lambda^2\phi^2 + \frac{1}{3}\nu\lambda^4\right) \\ &= \alpha_0 + \frac{2}{3}\alpha_2\phi^2 + \frac{\nu}{3(1+\nu)^2}\frac{\alpha_2^2}{\alpha_4}. \end{aligned} \quad (7.15)$$

Here we have used the above expression (7.12) for λ^2. Averaging over one period, we use $\langle\phi^2\rangle = \lambda^2(1 - \mathbf{E}(\nu)/\mathbf{K}(\nu))$, and again using (7.12) we find

$$\begin{aligned}\langle\Psi\rangle_{\rm GL}^{\rm crystal} &= \alpha_0 + \left(-\frac{\alpha_2^2}{4\alpha_4}\right)\left[\frac{4}{1+\nu}\left(\frac{2+\nu}{3(1+\nu)} - \frac{2}{3}\frac{\mathbf{E}(\nu)}{\mathbf{K}(\nu)}\right)\right] \\ &\equiv \alpha_0 + \left(-\frac{\alpha_2^2}{4\alpha_4}\right)F(\nu). \end{aligned} \quad (7.16)$$

Note that the function $F(\nu)$ is a smooth function interpolating monotonically between $F(0) = 0$ and $F(1) = 1$. We have written $\langle\Psi\rangle_{\rm GL}^{\rm crystal}$ like this in order to compare with the homogeneous ansatz: $\phi = \lambda$. Then

$$\langle\Psi\rangle_{\rm GL}^{\rm homogeneous} = \alpha_0 + \alpha_2\lambda^2 + \alpha_4\lambda^4. \quad (7.17)$$

Minimizing with respect to λ^2, we obtain the condition $\lambda^2 = -\alpha_2/(2\alpha_4)$, and at this minimum

$$\langle\Psi\rangle_{\rm GL}^{\rm homogeneous} = \alpha_0 + \left(-\frac{\alpha_2^2}{4\alpha_4}\right). \quad (7.18)$$

Therefore, we can write

$$\langle\Psi\rangle_{\rm GL}^{\rm homogeneous} - \langle\Psi\rangle_{\rm GL}^{\rm crystal} = \left(-\frac{\alpha_2^2}{4\alpha_4}\right)[1 - F(\nu)]. \quad (7.19)$$

An important observation is that at the values of $\nu = 1$ and $\nu = 0$, the minimized grand potential reduces to that of the homogeneous and the massless condensates [recall $\mathbf{E}/\mathbf{K}(\nu = 1) = 0$, $\mathbf{E}/\mathbf{K}(\nu = 0) = 1$]:

$$\langle\Psi\rangle_{\rm GL}^{\rm crystal}(\nu = 1) = \alpha_0 + \left(-\frac{\alpha_2^2}{4\alpha_4}\right) = \langle\Psi\rangle_{\rm GL}^{\rm homogenous}$$
$$\langle\Psi\rangle_{\rm GL}^{\rm crystal}(\nu = 0) = \alpha_0 = \langle\Psi\rangle_{\rm GL}^{\rm massless}. \quad (7.20)$$

This behavior is depicted in Fig. 10, where the grand potential of the crystal condensate lies between that of the massless and massive homogeneous phases, interpolating between them as a function of ν. Minimizing with respect to ν pushes us to the massive homogeneous phase in the blue region, but to the massless homogeneous phase in the white region. Thus, at this order of the GL expansion, even though the solution to the GL equation has the form of a crystalline condensate, the thermodynamic minimum is a constant condensate, either zero or nonzero, but always constant. We show in the next section that this picture changes significantly at the next order.

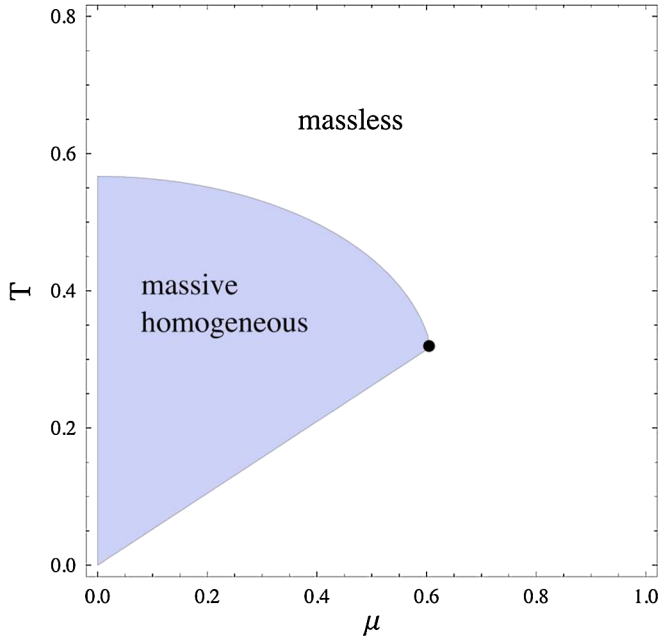

FIG. 10 (color online). The phase diagram of the GN_2 model, based on a Ginzburg-Landau expansion to the lowest nontrivial order: $O(\alpha_4)$. The blue region is the region in which the massive homogeneous condensate $\phi = \lambda$ has a lower grand potential. The white region is the region in which the homogeneous massless condensate $\phi = 0$ has a lower grand potential, or where only the massless condensate exists, because λ^2 in (7.12) is negative. These regions meet at the tricritical point: $T_{\rm tc} = 0.318$, $\mu_{\rm tc} = 0.608$.

2. Ginzburg-Landau expansion to $O(\alpha_6)$ for the $\mathbf{GN}_2$ model

Going to the next nontrivial order beyond the level defining the tricritical point, we expand the grand potential density in powers of the real condensate field ϕ and its derivatives (we drop the total derivative terms as these are not important for this argument):

$$\Psi_{\rm GL} = \alpha_0 + \alpha_2\phi^2 + \alpha_4(\phi^4 + \phi'^2) + \alpha_6(2\phi^6 + 10\phi^2\phi'^2 + \phi''^2). \quad (7.21)$$

The GL equation is now a fourth-order equation:

$$(\phi'''' - 10\phi^2\phi'' - 10\phi(\phi')^2 + 6\phi^5) + \frac{\alpha_4}{\alpha_6}(-\phi'' + 2\phi^3) + \frac{\alpha_2}{\alpha_6}\phi = 0. \quad (7.22)$$

The simplest solution is a homogeneous condensate, $\phi = \lambda$, with massless and massive solutions:

$$\lambda = 0 \qquad \text{(massless homogeneous phase)}$$
$$\lambda^4 + \frac{\alpha_4}{3\alpha_6}\lambda^2 + \frac{\alpha_2}{6\alpha_6} = 0 \Rightarrow \lambda_\pm^2 = -\frac{\alpha_4}{6\alpha_6}\left(1 \pm \sqrt{1 - \frac{6\alpha_2\alpha_6}{\alpha_4^2}}\right) \qquad \text{(massive homogeneous phase)}. \quad (7.23)$$

The general solution to (7.22) is very complicated, but we can use the inhomogeneous solution to the NLSE

$$\phi = \lambda\sqrt{\nu}\,\mathrm{sn}(\lambda x, \nu). \quad (7.24)$$

A similar idea was used in an analogous condensed matter model in [35]. This solution satisfies the nonlinear equations:

$$-\phi'' + 2\phi^3 = (1 + \nu)\lambda^2\phi$$
$$(\phi'''' - 10\phi^2\phi'' - 10\phi(\phi')^2 + 6\phi^5) = (\nu^2 + 4\nu + 1)\lambda^4\phi. \quad (7.25)$$

Thus, comparing with the GL equation (7.22), we see that ϕ satisfies the GL equation (7.22) provided we identify

$$\lambda^4 + \frac{\nu + 1}{(\nu^2 + 4\nu + 1)}\frac{\alpha_4}{\alpha_6}\lambda^2 + \frac{1}{(\nu^2 + 4\nu + 1)}\frac{\alpha_2}{\alpha_6} = 0. \quad (7.26)$$

This condition leads to two solutions

$$\lambda_{\pm}^2 = -\frac{\nu+1}{2(\nu^2+4\nu+1)}\frac{\alpha_4}{\alpha_6} \times\left(1\pm\left(1-\frac{4(\nu^2+4\nu+1)}{(\nu+1)^2}\frac{\alpha_2\alpha_6}{\alpha_4^2}\right)^{1/2}\right). \quad (7.27)$$

Evaluated on the crystalline solution, the grand potential is

$$\langle\Psi\rangle_{\rm GL} = \alpha_0 + \lambda^2\alpha_2\left(1-\frac{\mathbf{E}}{\mathbf{K}}\right) + \frac{\lambda^4\alpha_4}{3}\left(1+2\nu-(1+\nu)\frac{\mathbf{E}}{\mathbf{K}}\right) + \frac{\lambda^6\alpha_6}{5}\left(3\nu^2+6\nu+1-(\nu^2+4\nu+1)\frac{\mathbf{E}}{\mathbf{K}}\right). \quad (7.28)$$

This is just a function of T and μ (through the α's) and the elliptic parameter ν, because λ is given by the solutions in (7.27). We can therefore evaluate the grand potential throughout the (T, μ) plane and ask where it is lower than the grand potential of the homogeneous phase. The result is shown in Fig. 11, which shows the existence of a crystalline phase in a small region in the vicinity of the tricritical point. This is a region in which the grand potential of the crystalline condensate is lower than that of the massless or massive homogeneous condensate. On the upper edge, $\nu = 0$ and the scale of the crystalline condensate vanishes as it reduces to a massless phase; on the lower edge, $\nu = 1$, and the period of the crystalline condensate diverges as it reduces to a homogeneous massive phase. The form of this region matches very well with the full crystalline region, near the tricritical point, as shown by the close-up view in Fig. 12. Going to higher orders of the GL expansion, this crystalline region grows, and eventually covers the entire region given by the exact numerics [16].

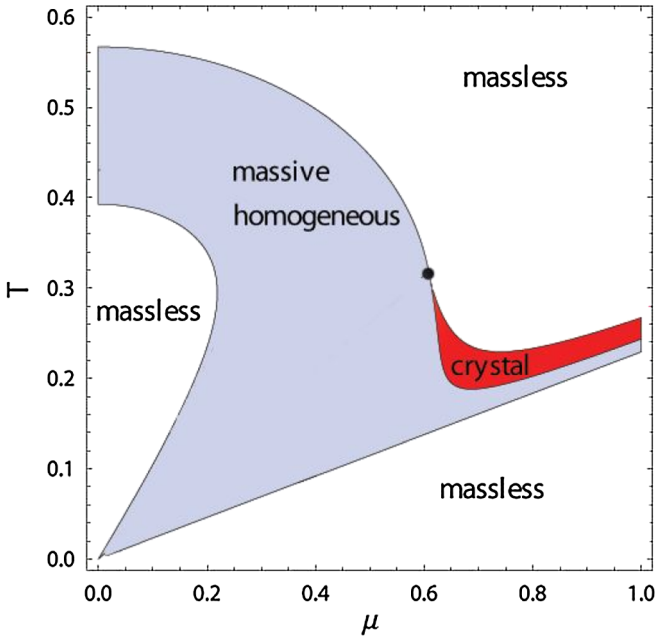

FIG. 11 (color online). The phase diagram of the GN_2 model, based on a Ginzburg-Landau expansion to the lowest nontrivial order: $O(\alpha_6)$. The light (blue) shaded region in which the homogeneous condensate $\phi = \lambda$ has the lowest grand potential. The dark (red) shaded region is the region in which the crystalline condensate (7.24) has the lowest grand potential. In the remaining (white) region, the homogeneous massless condensate $\phi = 0$ has the lowest grand potential. Note that the crystal phase region begins at the tricritical point: $T_{\rm tc} = 0.318$, $\mu_{\rm tc} = 0.608$. A close-up of this region is shown in Fig. 12.

B. Ginzburg-Landau expansion for the NJL_2 model

In contrast to the GN_2 model, the α_3 term in (7.1) is present in the GL expansion of the NJL_2 model, as the condensate Δ is complex. The "tricritical" point is defined as the point where the two lowest nontrivial coefficients, $\alpha_2(T, \mu)$ and $\alpha_3(T, \mu)$, vanish:

$$\alpha_2(T,\mu) = \alpha_3(T,\mu) = 0 \Rightarrow T_{\rm tc} = 0.566, \qquad \mu_{\rm tc} = 0. \quad (7.29)$$

1. Ginzburg-Landau expansion to $O(\alpha_3)$ for the NJL_2 model

The first nontrivial order, to $O(\alpha_3)$, leads to the GL equation

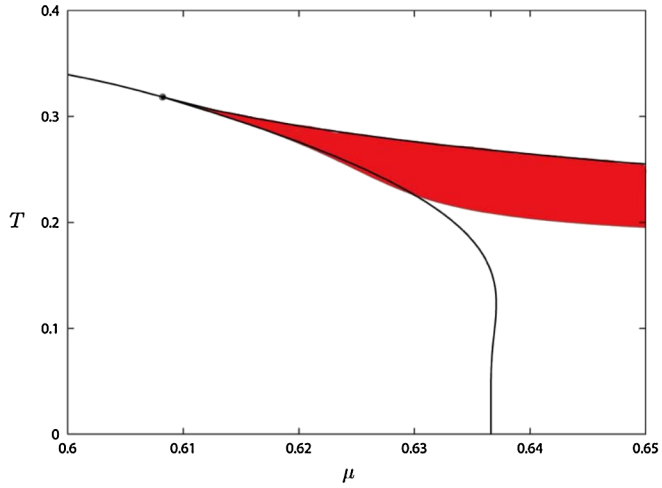

FIG. 12 (color online). A close-up view of the crystalline region in the phase diagram of the GN_2 model, near the tricritical point, based on a Ginzburg-Landau expansion to the lowest nontrivial order: $O(\alpha_6)$. The red shaded region is the crystalline region seen at this order of the GL expansion, while the solid black lines mark the edges of the true crystalline region found numerically from the exact grand potential [16]. The agreement is excellent near the tricritical point and near the LOFF boundary with the massless phase.

$$\Delta' - i\frac{\alpha_2}{\alpha_3}\Delta = 0 \Rightarrow \Delta = \lambda \exp\left[i\frac{\alpha_2}{\alpha_3}x\right]. \tag{7.30}$$

But for this solution, even though this condensate is crystalline, the grand potential is $\langle\Psi\rangle_{\rm GL} = \alpha_0$. Thus, the phase diagram is simply that of a massless phase. The only thing we learn at this level of the GL expansion is the existence of the tricritical point at $T = 0.5669$ and $\mu = 0$. This is analogous to the situation of the GL expansion of the GN_2 model to its first nontrivial order, $O(\alpha_4)$, where the solution of the GL equation has a crystalline form, but this crystalline condensate does not appear in the phase diagram at that order, as discussed in Sec VII A 1.

2. Ginzburg-Landau expansion to $O(\alpha_4)$ for the NJL_2 model

Going to the next nontrivial order beyond the level defining the tricritical point, namely, to $O(\alpha_4)$, we obtain the GL equation of NLSE form in (7.5). Adapting the solution in Sec. II A, we can write the general solution as

$$\Delta = -\lambda\frac{\sigma(\lambda x + i\mathbf{K}' - i\theta/2)}{\sigma(\lambda x + i\mathbf{K}')\sigma(i\theta/2)}\exp[i\lambda x(-i\zeta(i\theta/2) + q) + i\theta\eta_3/2] \tag{7.31}$$

which satisfies

$$-\Delta'' + 2\Delta|\Delta|^2 = -2iq\lambda\Delta' + \lambda^2(-3\mathcal{P}(i\theta/2) - q^2)\Delta. \tag{7.32}$$

Identifying the terms with the NLSE equation we deduce $q = \frac{\alpha_3}{2\lambda\alpha_4}$, and λ must satisfy

$$\lambda^2 = \left(-\frac{\alpha_2}{2\alpha_4}\left[1 - \frac{\alpha_3^2}{4\alpha_2\alpha_4}\right]\right)\left(\frac{2}{-3\mathcal{P}(i\theta/2)}\right). \tag{7.33}$$

Note that $(-\mathcal{P}(i\theta/2)) \geq 0$. Thus, this inhomogeneous crystal condensate only makes sense in regions of the (T, μ) plane where $(-\frac{\alpha_2}{\alpha_4}[1 - \frac{\alpha_3^2}{4\alpha_2\alpha_4}]) \geq 0$.

Now evaluating the averaged potential on this solution, we find

$$\begin{aligned}\langle\Psi\rangle_{\rm GL}^{\rm crystal} &= \alpha_0 + \left[-\frac{\alpha_2^2}{4\alpha_4}\left(1 - \frac{\alpha_3^2}{4\alpha_2\alpha_4}\right)^2\right] \\ &\quad\times\left[\frac{4}{9}\left(1 + \frac{\nu^2 - \nu + 1}{9\mathcal{P}(i\theta/2)^2} + \frac{2}{\mathcal{P}(i\theta/2)}\frac{\eta}{\mathbf{K}}\right)\right] \\ &\equiv \alpha_0 + \left[-\frac{\alpha_2^2}{4\alpha_4}\left(1 - \frac{\alpha_3^2}{4\alpha_2\alpha_4}\right)^2\right]F(\nu,\theta)\end{aligned} \tag{7.34}$$

which should be compared with the corresponding GN_2 expression (7.16). (Indeed, setting $\theta = 2\mathbf{K}'$, and $\alpha_3 = 0$, we recover the GN_2 formulas). We note that $0 \leq F(\nu, \theta) \leq 1$. We now compare the averaged potential for the crystal with that obtained from a spiral ansatz:

$$\Delta^{\rm spiral} = \lambda e^{2iqx}. \tag{7.35}$$

With this spiral ansatz we find

$$\langle\Psi\rangle_{\rm GL}^{\rm spiral} = \alpha_0 + \lambda^2\alpha_2 - 2q\lambda^2\alpha_3 + (\lambda^4 + 4q^2\lambda^2)\alpha_4. \tag{7.36}$$

Minimizing with respect to q we find $q = \alpha_3/\alpha_4$, and further minimizing with respect to λ^2 we find

$$\lambda^2 = \left(-\frac{\alpha_2}{2\alpha_4}\left[1 - \frac{\alpha_3^2}{4\alpha_2\alpha_4}\right]\right) \tag{7.37}$$

which should be compared with (7.33). Furthermore, evaluating the averaged potential on this spiral condensate we find

$$\langle\Psi\rangle_{\rm GL}^{\rm spiral} = \alpha_0 + \left[-\frac{\alpha_2^2}{4\alpha_4}\left(1 - \frac{\alpha_3^2}{4\alpha_2\alpha_4}\right)^2\right] \tag{7.38}$$

which should be compared with (7.34).

Now we combine this expression with the positivity condition on λ^2 in (7.12) to obtain the phase diagram in Fig. 13. Just as in the GN_2 case, here in the NJL_2 model, by going one step beyond the first nontrivial order of the GL expansion (i.e., one step beyond the order that defines the tricritical point) we see the appearance of a crystalline phase in the phase diagram, in the region near the tricritical point. For the NJL_2 model, the condensate of this crystalline phase, derived from this GL approach to this order, has the form of the chiral spiral after minimization of the grand potential. This Ginzburg-Landau analysis confirms once again that the chiral spiral is the thermodynamically pre-

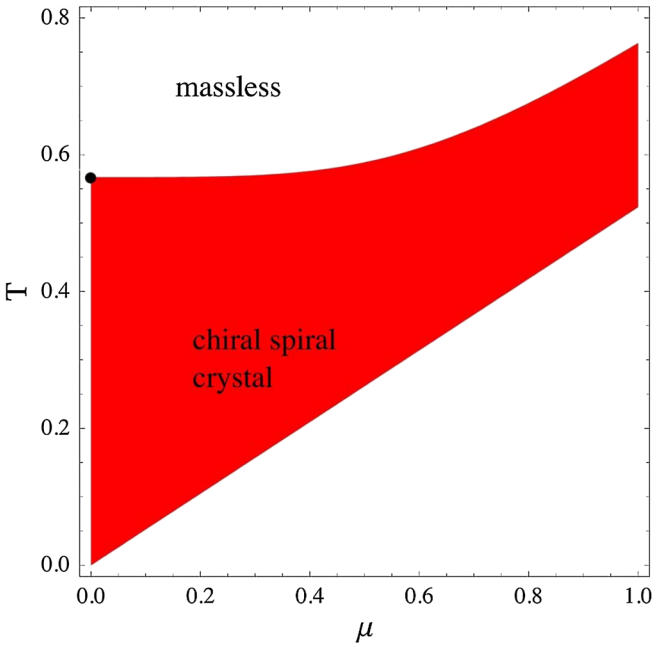

FIG. 13 (color online). The phase diagram of the NJL_2 model, based on a Ginzburg-Landau expansion to $O(\alpha_4)$. The (red) shaded region is the region in which the spiral condensate (4.1) has a lower grand potential. In the remaining regions the massless condensate $\Delta = 0$ is preferred.

ferred form of the inhomogeneous condensate, in the applicable part of the phase diagram. The pattern is fairly clear: going to higher orders of the GL expansion, the crystalline region grows, and eventually covers the entire region given by the exact numerics, as shown in Fig. 5.

VII. CONCLUSIONS

We have used the exact crystalline solutions to the inhomogeneous gap equation of the NJL_2 model, found in [13,14], to probe the thermodynamic phase diagram of the NJL_2 and GN_2 models at finite density and temperature. Using a combination of exact, numerical and Ginzburg-Landau approaches, we have shown that for the NJL_2 model the thermodynamically preferred condensate in the region $T < T_c$ is the helical chiral spiral of [15]. The same methods have been applied to the GN_2 model, confirming previous numerical results [16]. A key new idea in our analysis is the exploitation of the behavior of the grand potential under the rescaling and phase rotation transformations (3.1), which affect the renormalized grand potential as in (3.16). This observation greatly facilitates the minimization of the renormalized grand potential with respect to the parameters λ and q. We are also able to trace in a very explicit manner the consequences for the phase diagram of the fact that the GN_2 model has a discrete chiral symmetry, while the NJL_2 model has a continuous chiral symmetry. These one dimensional models are somewhat special, due to the rich integrability structure underlying their gap equation. So, we studied these models also using the Ginzburg-Landau approach, which does not necessarily rely on this integrability structure. We found that in both the NJL_2 and GN_2 models the crystalline region appears at the order of the Ginzburg-Landau expansion *one step beyond* the first nontrivial order, which is used to identify the relevant tricritical point. It would be interesting to study this point systematically in higher dimensional models, where the search for crystalline phases is considerably more difficult [21,35–37]. It would also be interesting to study the NJL_2 system on the lattice, complementing the GN_2 work of [17,18], and the recent Monte Carlo formulations in [38–40]. Other interesting effects include the study of an isospin chemical potential [41], and going beyond the leading large N approximation [42].

ACKNOWLEDGMENTS

G. B. and G. D. thank the DOE for support through Grant No. DE-FG02-92ER40716, and G. D. thanks the Institut für Theoretische Physik at Erlangen for support during a visit. We are grateful to F. Correa, V. Enolskii, F. Gesztesy, and D. Nickel for helpful comments and suggestions.

[1] R. Peierls, *The Quantum Theory of Solids* (Oxford University, New York, 1955).
[2] P. G. de Gennes, *Superconductivity of Metals and Alloys* (Addison-Wesley, Redwood City, California, 1989).
[3] Y. Nambu and G. Jona-Lasinio, Phys. Rev. **122**, 345 (1961); Phys. Rev. **124**, 246 (1961).
[4] K. Rajagopal and F. Wilczek, in *At the Frontier of Particle Physics/Handbook of QCD*, edited by M. Shifman (World Scientific, Singapore, 2001); arXiv:hep-ph/0011333.
[5] M. G. Alford, J. A. Bowers, and K. Rajagopal, Phys. Rev. D **63**, 074016 (2001).
[6] R. Casalbuoni and G. Nardulli, Rev. Mod. Phys. **76**, 263 (2004).
[7] L. McLerran and R. D. Pisarski, Nucl. Phys. **A796**, 83 (2007); Y. Hidaka, L. D. McLerran, and R. D. Pisarski, Nucl. Phys. **A808**, 117 (2008).
[8] L. Y. Glozman and R. F. Wagenbrunn, Phys. Rev. D **77**, 054027 (2008); arXiv:0805.4799.
[9] D. J. Gross and A. Neveu, Phys. Rev. D **10**, 3235 (1974).
[10] R. F. Dashen, B. Hasslacher, and A. Neveu, Phys. Rev. D **12**, 2443 (1975).
[11] S. S. Shei, Phys. Rev. D **14**, 535 (1976).
[12] J. Feinberg and A. Zee, Phys. Rev. D **56**, 5050 (1997); in *Multiple Facets of Quantization and Supersymmetry*, edited by M. Olshanetsky *et al.* (World Scientific, Singapore, 2002).
[13] G. Basar and G. V. Dunne, Phys. Rev. Lett. **100**, 200404 (2008).
[14] G. Basar and G. V. Dunne, Phys. Rev. D **78**, 065022 (2008).
[15] V. Schön and M. Thies, Phys. Rev. D **62**, 096002 (2000); V. Schön and M. Thies in *At the Frontier of Particle Physics*, edited by M. Shifman (World Scientific, Singapore, 2001), Vol. 3.
[16] M. Thies, Phys. Rev. D **69**, 067703 (2004); J. Phys. A **39**, 12707 (2006).
[17] P. de Forcrand and U. Wenger, Proc. Sci., LAT2006 (2006) 152.
[18] F. Karsch, J. B. Kogut, and H. W. Wyld, Nucl. Phys. **B280**, 289 (1987).
[19] J. L. Davis, M. Gutperle, P. Kraus, and I. Sachs, J. High Energy Phys. 10 (2007) 049.
[20] B. Bringoltz, J. High Energy Phys. 03 (2007) 016; arXiv:0901.4035.
[21] D. Nickel and M. Buballa, Phys. Rev. D **79**, 054009 (2009); D. Nickel, arXiv:0902.1778.
[22] F. Karbstein and M. Thies, Phys. Rev. D **75**, 025003 (2007).
[23] U. Wolff, Phys. Lett. **157B**, 303 (1985).
[24] T. F. Treml, Phys. Rev. D **39**, 679 (1989).
[25] A. Neveu and N. Papanicolaou, Commun. Math. Phys. **58**, 31 (1978).

[26] F. Gesztesy and H. Holden, *Soliton Equations and their Algebro-Geometric Solutions* (Cambridge University Press, Cambridge, England, 2003).
[27] F. Correa, G. V. Dunne, and M. Plyushchay, arXiV:0904.2768.
[28] E. Witten, Nucl. Phys. **B145**, 110 (1978); **B149**, 285 (1979).
[29] I. K. Affleck, Phys. Lett. **109B**, 307 (1982).
[30] I. Kosztin, S. Kos, M. Stone, and A. J. Leggett, Phys. Rev. B **58**, 9365 (1998); S. Kos and M. Stone, Phys. Rev. B **59**, 9545 (1999).
[31] G. Eilenberger, Z. Phys. **214**, 195 (1968).
[32] L. A. Dickey, *Soliton Equations and Hamiltonian Systems* (World Scientific, Singapore, 1991).
[33] D. F. Lawden, *Elliptic Functions and Applications* (Springer-Verlag, New York, 1980).
[34] J. Feinberg, Ann. Phys. (N.Y.) **309**, 166 (2004).
[35] A. I. Buzdin and H. Kachkachi, Phys. Lett. A **225**, 341 (1997).
[36] R. Casalbuoni *et al.*, Phys. Lett. B **627**, 89 (2005); **634**, 565(E) (2006).
[37] M. Mannarelli, K. Rajagopal, and R. Sharma, Phys. Rev. D **73**, 114012 (2006).
[38] C. Gattringer, V. Hermann, and M. Limmer, Phys. Rev. D **76**, 014503 (2007).
[39] U. Wolff, Nucl. Phys. **B789**, 258 (2008).
[40] K. Langfeld, G. Dunne, H. Gies, and K. Klingmuller, Proc. Sci., LAT2007 (2007) 202.
[41] D. Ebert, K. G. Klimenko, A. V. Tyukov, and V. C. Zhukovsky, Phys. Rev. D **78**, 045008 (2008); D. Ebert and K. G. Klimenko, arXiv:0902.1861.
[42] J. L. Kneur, M. B. Pinto, and R. O. Ramos, Braz. J. Phys. **31**, 258 (2007); J. L. Kneur, M. B. Pinto, and R. O. Ramos, Int. J. Mod. Phys. E **16**, 2798 (2007).